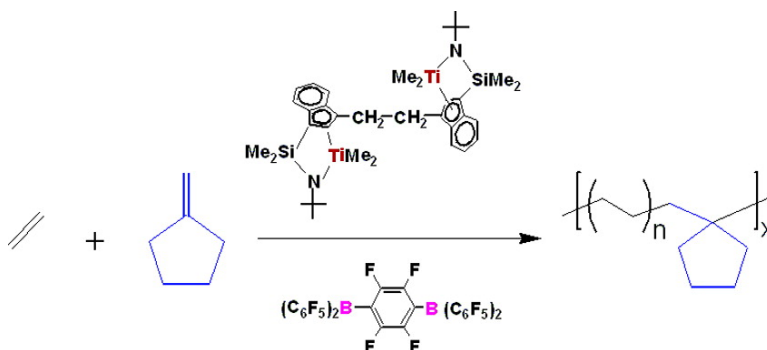


Coordination Copolymerization of Severely Encumbered Isoalkenes with Ethylene: Enhanced Enchainment Mediated by Binuclear Catalysts and Cocatalysts

Hongbo Li, Liting Li, David J. Schwartz, Matthew V. Metz,
 Tobin J. Marks, Louise Liable-Sands, and Arnold L. Rheingold

J. Am. Chem. Soc., **2005**, 127 (42), 14756-14768 • DOI: 10.1021/ja052995x • Publication Date (Web): 29 September 2005

Downloaded from <http://pubs.acs.org> on March 25, 2009



More About This Article

Additional resources and features associated with this article are available within the HTML version:

- Supporting Information
- Links to the 10 articles that cite this article, as of the time of this article download
- Access to high resolution figures
- Links to articles and content related to this article
- Copyright permission to reproduce figures and/or text from this article

[View the Full Text HTML](#)

Coordination Copolymerization of Severely Encumbered Isoalkenes with Ethylene: Enhanced Enchainment Mediated by Binuclear Catalysts and Cocatalysts

Hongbo Li,[†] Liting Li,[†] David J. Schwartz,[†] Matthew V. Metz,[†] Tobin J. Marks,^{*,†}
Louise Liabe-Sands,[‡] and Arnold L. Rheingold[‡]

Contribution from the Department of Chemistry, Northwestern University, Evanston, Illinois 60208-3113, and Department of Chemistry and Biochemistry, University of California, San Diego, La Jolla, California 92093-0332

Received May 7, 2005; E-mail: t-marks@northwestern.edu

Abstract: This contribution describes the implementation of the binuclear organotitanium “constrained geometry catalysts” (CGCs), $(\mu\text{-CH}_2\text{CH}_2\text{-3,3'})\{(\eta^5\text{-indenyl})[1\text{-Me}_2\text{Si}(\text{BuN})](\text{TiMe}_2)_2\}_2[\text{EBICGC}(\text{TiMe}_2)_2; \mathbf{Ti}_2]$ and $(\mu\text{-CH}_2\text{-3,3'})\{(\eta^5\text{-indenyl})[1\text{-Me}_2\text{Si}(\text{BuN})](\text{TiMe}_2)_2\}_2[\text{MBICGC}(\text{TiMe}_2)_2; \mathbf{C1-Ti}_2]$, in combination with the bifunctional bisborane activator $1,4\text{-(C}_6\text{F}_5)_2\text{BC}_6\text{F}_4\text{B(C}_6\text{F}_5)_2$ (\mathbf{BN}_2) in ethylene + olefin copolymerization processes. Specifically examined are the classically poorly responsive 1,1-disubstituted comonomers, methylenecyclopentane (**C**), methylenecyclohexane (**D**), 1,1,2-trisubstituted 2-methyl-2-butene (**E**), and isobutene (**F**). For the first three comonomers, this represents the first report of their incorporation into a polyethylene backbone via a coordination polymerization process. **C** and **D** are incorporated via a ring-unopened pathway, and **E** is incorporated via a novel pathway involving 2-methyl-1-butene enchainment in the copolymer backbone. In ethylene copolymerization, $\mathbf{Ti}_2 + \mathbf{BN}_2$ enchains ~ 2.5 times more **C**, ~ 2.5 times more **D**, and ~ 2.3 times more **E** than the mononuclear catalyst analogue $[1\text{-Me}_2\text{Si}(3\text{-ethylindenyl})\text{-}(\text{BuN})\text{TiMe}_2$ (\mathbf{Ti}_1) + $\text{B(C}_6\text{F}_5)_3$ (\mathbf{BN}) under identical polymerization conditions. Polar solvents are found to weaken the catalyst–cocatalyst ion pairing, thus influencing the comonomer enchainment selectivity.

Introduction

Enzymes achieve superior reactivity and selectivity, in part due to their efficacy in creating high local reagent concentrations and special, conformationally advantageous active site–substrate proximities/interactions.¹ In this regard, the possibility of unique and more efficient catalytic transformations based on cooperative effects between adjacent active centers in multinuclear transition metal complexes is currently under intense investigation.² For single-site olefin polymerization catalysts,^{3–5} we recently

reported⁴ that the $\text{—CH}_2\text{CH}_2\text{—}$ bridged bimetallic catalysts, \mathbf{Ti}_2 and \mathbf{Zr}_2 , as well as binuclear cocatalysts, \mathbf{B}_2 and \mathbf{BN}_2 ,^{4,6} exhibit significant nuclearity effects in terms of chain branch formation and comonomer enchainment selectivity versus their mononuclear counterparts (Chart 1). Generally, CGCZr catalysts

[†] Northwestern University.

[‡] University of California, San Diego.

- (1) (a) Collman, J. P.; Boulatov, R.; Sunderland, C. J.; Fu, L. *Chem. Rev.* **2004**, *104*, 561–588. (b) Krishnan, R.; Voo, J. K.; Riordan, C. G.; Zahkarov, L.; Rheingold, A. L. *J. Am. Chem. Soc.* **2003**, *125*, 4422–4423. (c) Bruce, T. C. *Acc. Chem. Res.* **2002**, *35*, 139–148. (d) Bruce, T. C.; Benkovic, S. J. *Biochemistry* **2000**, *39*, 6267–6274 and references therein. (e) O'Brien, D. P.; Entress, R. M. N.; Matthew, A. C.; O'Brien, S. W.; Hopkinson, A.; Williams, D. H. *J. Am. Chem. Soc.* **1999**, *121*, 5259–5265. (f) Carazo-Salas, R. E.; Guarguaglini, G.; Gruss, O. J.; Segref, A.; Karsenti, E.; Mattaj, L. W. *Nature* **1999**, *400*, 178–181. (g) Menger, F. M. *Acc. Chem. Res.* **1993**, *26*, 206–212 and references therein. (h) Page, M. I. In *The Chemistry of Enzyme Action*; Page, M. I., Ed.; Elsevier: New York, 1984; pp 1–54.
- (2) (a) Sammis, G. M.; Danjo, H.; Jacobsen, E. N. *J. Am. Chem. Soc.* **2004**, *126*, 9928–9929. (b) Moore, D. R.; Cheng, M.; Lobkovsky, E. B.; Coates, G. W. *J. Am. Chem. Soc.* **2003**, *125*, 11911–11924. (c) Trost, B. M.; Mino, T. *J. Am. Chem. Soc.* **2003**, *125*, 2410–2411. (d) Jacobsen, E. N. *Acc. Chem. Res.* **2000**, *33*, 421–431. (e) Molenveld, P.; Engbersen, J. F. J.; Reinhoudt, D. N. *Chem. Soc. Rev.* **2000**, *29*, 75–86. (f) Konler, R. G.; Karl, J.; Jacobsen, E. N. *J. Am. Chem. Soc.* **1998**, *120*, 10780–10781. (g) Molenveld, P.; Kapsabelis, S.; Engbersen, J. F. J.; Reinhoudt, D. N. *J. Am. Chem. Soc.* **1997**, *119*, 2948–2949. (h) Mathews, R. C.; Howell, D. H.; Peng, W.-J.; Train, S. G.; Treleaven, W. D.; Stanley, G. G. *Angew. Chem., Int. Ed. Engl.* **1996**, *35*, 2253–2256. (i) Sawamura, M.; Sudoh, M.; Ito, Y. *J. Am. Chem. Soc.* **1996**, *118*, 3309–3310.

- (3) For recent reviews of single-site olefin polymerization, see: (a) Kaminsky, W. *J. Polym. Sci., Part B: Polym. Chem.* **2004**, *42*, 3911–3921. (b) Gibson, V. C.; Spitzmesser, S. K. *Chem. Rev.* **2003**, *103*, 283–316. (c) Pedeutour, J.-N.; Radhakrishnan, K.; Cramail, H.; Deffieux, A. *Macromol. Rapid Commun.* **2001**, *22*, 1095–1123. (d) Gladysz, J. A. *Chem. Rev.* **2000**, *100* (special issue on Frontiers in Metal-Catalyzed Polymerization). (e) Marks, T. J.; Stevens, J. C. *Top. Catal.* **1999**, *15*, and references therein. (f) Britovsek, G. J. P.; Gibson, V. C.; Wass, D. F. *Angew. Chem., Int. Ed.* **1999**, *38*, 428–447. (g) Kaminsky, W.; Arndt, M. *Adv. Polym. Sci.* **1997**, *127*, 144–187. (h) Bochmann, M. *J. Chem. Soc., Dalton Trans.* **1996**, 255–270. (i) Brintzinger, H.-H.; Fischer, D.; Mülhaupt, R.; Rieger, B.; Waymouth, R. M. *Angew. Chem., Int. Ed. Engl.* **1995**, *34*, 1143–1170. (j) *Catalyst Design for Tailor-Made Polyolefins*; Soga, K., Terano, M., Eds.; Elsevier: Tokyo, 1994. (k) Marks, T. J. *Acc. Chem. Res.* **1992**, *25*, 57–65.
- (4) For studies of binuclear metallocenes, see: (a) Li, H.; Li, L.; Marks, T. J. *Angew. Chem., Int. Ed.* **2004**, *37*, 4937–4940. (b) Wang, J.; Li, H.; Guo, N.; Li, L.; Stern, C. L.; Marks, T. J. *Organometallics* **2004**, *23*, 5112–5114. (c) Guo, N.; Li, L.; Marks, T. J. *J. Am. Chem. Soc.* **2004**, *126*, 6542–43. (d) Li, H.; Li, L.; Marks, T. J.; Liabe-Sands, L.; Rheingold, A. L. *J. Am. Chem. Soc.* **2003**, *125*, 10788–10789. (e) Noh, S. K.; Lee, J.; Lee, D. *J. Organomet. Chem.* **2003**, *667*, 53–60. (f) Li, L.; Metz, M. V.; Li, H.; Chen, M.-C.; Marks, T. J.; Liabe-Sands, L.; Rheingold, A. L. *J. Am. Chem. Soc.* **2002**, *124*, 12725–12741. (g) Abramo, G. P.; Li, L.; Marks, T. J. *J. Am. Chem. Soc.* **2002**, *124*, 13966–13967. (h) Green, M. L. H.; Popham, N. H. *J. Chem. Soc., Dalton Trans.* **1999**, 1049–1059 and references therein. (i) Spaleck, W.; Kuber, F.; Bachmann, B.; Fritze, C.; Winter, A. *J. Mol. Catal. A: Chem.* **1998**, *128*, 279–287. (j) Yan, X.; Chernega, A.; Green, M. L. H.; Sanders, J.; Souter, J.; Ushioda, T. *J. Mol. Catal. A: Chem.* **1998**, *128*, 119–141. (k) Soga, K.; Ban, H. T.; Uozumi, T. *J. Mol. Catal. A: Chem.* **1998**, *128*, 273–278. (l) Bochmann, M.; Cuenca, T.; Hardy, D. T. *J. Organomet. Chem.* **1994**, *484*, C10–C12.

Chart 1

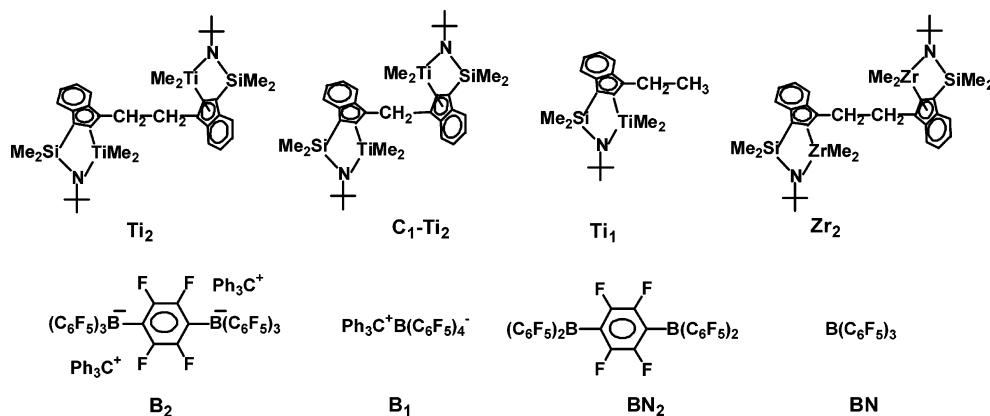
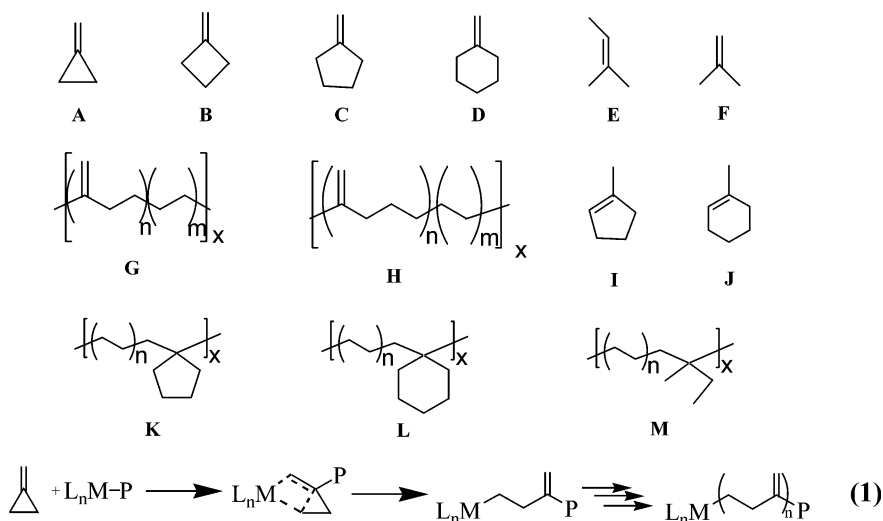


Chart 2



produce low- M_w polyolefins with low activity and with low α -olefin coenchainment efficiency,⁵ while CGCTi catalysts produce high- M_w polyolefins with high activity and high α -olefin coenchainment efficiency. In a previous communication,^{4d} we reported that the binuclear organotitanium catalyst Ti_2 + binuclear activators significantly enhances incorporation of sterically encumbered isobutene (F) in ethylene copolymeriza-

tions. This observation raises the intriguing question of just how general this unusual selectivity pattern is and whether it can be extended to even more severely encumbered monomers. Herein we report a full discussion of the implementation of binuclear catalysts and cocatalysts in such copolymerization processes, including results with a new $-CH_2-$ bridged binuclear catalyst ($C1-Ti_2$).

We previously reported an unusual example of a d^0/f^n metallocene-mediated β -alkyl elimination process: ring-opening Ziegler polymerization (ROZP; eq 1 in Chart 2)⁷ of the strained methylenecycloalkanes, methylenecyclopropane (A), and methylenecyclobutane (B) in which sequential double-bond insertions and β -alkyl shift ring openings afford polyolefins with *exo*-methylene functionalities along the backbone (G and H). For those monomers having less or no ring strain in cases such as methylenecyclopentane (C) and methylenecyclohexane (D), isomerization to the thermodynamically more stable internal cycloolefins (I and J, respectively) is known to occur under reaction conditions mediated by a variety of mononuclear d^0/f^n metallocene catalysts.

- (5) (a) Chum, P. S.; Kruper, W. J.; Guest, M. J. *Adv. Mater.* **2000**, *12*, 1759–1767. (b) McKnight, A. L.; Waymouth, R. M. *Chem. Rev.* **1998**, *98*, 2587–2598. (c) Harrison, D.; Coulter, I. M.; Wang, S. T.; Nistala, S.; Kuntz, B. A.; Pigeon, M.; Tian, J.; Collins, S. *J. Mol. Catal. A: Chem.* **1998**, *128*, 65–77. (d) Soga, K.; Uozumi, T.; Nakamura, S.; Toneri, T.; Teranishi, T.; Sano, T.; Arai, T.; Shiono, T. *Macromol. Chem. Phys.* **1996**, *197*, 4237–4251. (e) Devore, D. D.; Timmers, F. J.; Hasha, D. L.; Rosen, R. K.; Marks, T. J.; Deck, P. A.; Stern, C. L. *Organometallics* **1995**, *14*, 3132–3134. (f) Lai, S. Y.; Wilson, J. R.; Knight, G. W.; Stevens, J. C. WO-93/08221, 1993. (g) Canich, J. M.; Hlatky, G. G.; Turner, H. W. *PCT Appl. WO-92/00333*, 1992; Canich, J. M. *Eur. Patent Appl.* EP 420 436-A1, 1991 (Exxon Chemical Co.). (h) Devore, D. D. European Patent Application EP-514-828-A1, November 25, 1992.
- (6) Similar bifunctional cocatalysts: (a) Lewis, S. P.; Henderson, L. D.; Chandler, B. D.; Parvez, M.; Piers, W. E.; Collins, S. *J. Am. Chem. Soc.* **2005**, *127*, 46–47. (b) Lewis, S. P.; Taylor, N. J.; Piers, W. E.; Collins, S. *J. Am. Chem. Soc.* **2003**, *125*, 14686–14687. (c) Metz, M. V.; Schwartz, D. J.; Stern, C. L.; Marks, T. J.; Nickias, P. N. *Organometallics* **2002**, *21*, 4159–4168. (d) Lancaster, S. J.; Rodriguez, A.; Lara-Sanchez, A.; Hannant, M. D.; Walker, D. A.; Hughes, D. H.; Bochmann, M. *Organometallics* **2002**, *21*, 451–453. (e) McAdon, M. H.; Nickias, P. N.; Marks, T. J.; Schwartz, D. J. WO9906413A1, February 11, 1999. (f) Metz, M. V.; Schwartz, D. J.; Stern, C. L.; Nickias, P. N.; Marks, T. J. *Angew. Chem., Int. Ed.* **2000**, *39*, 1312–1316. (g) Williams, V. C.; Piers, W. E.; Clegg, W.; Elsegood, M. R. J.; Collins, S.; Marder, T. B. *J. Am. Chem. Soc.* **1999**, *121*, 3244–3245. (h) Jia, L.; Yang, X.; Stern, C. L.; Marks, T. J. *Organometallics* **1997**, *16*, 842–857.

- (7) (a) Jensen, T. R.; O'Donnell, J. J., III; Marks, T. J. *Organometallics* **2004**, *23*, 740–754. (b) Jia, L.; Yang, X. M.; Seyam, A. M.; Albert, I. D. L.; Fu, P. F.; Yang, S. T.; Marks, T. J. *J. Am. Chem. Soc.* **1996**, *118*, 7900–7913. (c) Jia, L.; Yang, X. M.; Yang, S. T.; Marks, T. J. *J. Am. Chem. Soc.* **1996**, *118*, 1547–1548. (d) Yang, X. M.; Seyam, A. M.; Fu, P. F.; Marks, T. J. *Macromolecules* **1994**, *27*, 4625–4626. (e) Yang, X. M.; Jia, L.; Marks, T. J. *J. Am. Chem. Soc.* **1993**, *115*, 3392–3393.

Several methylenecycloalkane derivatives have been reported to undergo polymerization/copolymerization via *ring-unopened* pathways, yielding polymers with saturated hydrocarbon rings appended to the polyolefin backbone.^{7a,8} Such an architecture of saturated hydrocarbon rings arrayed along a polymer chain is expected to afford significantly altered physical properties because the bulky cycloalkane rings should frustrate the tendency to coil tightly and should, thus, increase the average chain length between entanglements.^{9–11} Intensive research efforts have focused on producing this type of polymeric product,^{10,11} and the saturated hydrocarbon rings are typically created in the polymer backbone via heterogeneous hydrogenation of aromatic-functionalized macromolecules, such as polystyrene^{11b–d} and polyindene.^{11a} Compared with their unsaturated precursors, saturated ring-functionalized polymers should have lower dielectric constants, lower refractive indices, lower water absorption, and greater optical transparency.^{10b} However, such inefficient two-step processes require relatively harsh hydrogenation conditions and frequently suffer from incomplete hydrogenation and chain scission. For these reasons, a single-step homogeneous catalytic polymerization process represents an attractive approach to accessing this challenging macromolecular structure class.³ Nevertheless, in the methylenecycloalkane family, only methylenecyclopropane derivatives have so far been reported to be effective comonomers for this type of polymerization, reflecting the highly constricted geometries of three-membered rings, which presumably reduce steric hindrance to C=C enchainment. Since the substantial strain of the three-membered ring can potentially compromise polymer stability, monomers such as **C** or **D** with minimal ring strain (6.5 and 0 kcal/mol for **C** and **D**, respectively), when incorporated into a polyethylene chain in a ring-unopened geometry, are expected to enhance the polymer thermal and chemical stability and promote the aforementioned entanglement properties.^{7a,10}

Here, we report that with coordinatively more open CGCTi⁺ catalysts, sterically hindered monomers **C** and **D**, can now be incorporated into the polyethylene backbone in a ring-unopened fashion to afford macromolecules **K** and **L**, respectively, rather than simply undergoing double-bond migration. More interestingly, the even more sterically encumbered 1,1,2-trisubstituted monomer 2-methyl-2-butene (**E**) can also be enchainment to form copolymer **M**. We report here the synthesis, characterization, and ethylene/isoalkene copolymerization characteristics of the catalysts which efficiently effect these transformations—

bimetallic “constrained geometry complexes” (CGC) (μ -CH₂-CH₂-3,3') $\{(\eta^5$ -indenyl)[1-Me₂Si(BuN)](TiMe₂)₂ (**Ti₂**) and (μ -CH₂-3,3') $\{(\eta^5$ -indenyl)[1-Me₂Si(BuN)](TiMe₂)₂ (**C1–Ti₂**), the monometallic analogue [1-Me₂Si(3-ethylindenyl)(BuN)]TiMe₂ (**Ti₁**) for comparative purposes, and the new binuclear bisborane cocatalyst 1,4-(C₆F₅)₂BC₆F₄B(C₆F₅)₂ (**BN₂**). The ethylene + **C**, ethylene + **D**, and ethylene + **E** copolymerization characteristics with various catalysts/cocatalyst combinations are then examined in detail. It will be seen that this new family of CGCTi catalysts can efficiently incorporate these sterically encumbered comonomers into polyethylene backbones, and that the consequence of increasing catalyst and cocatalyst nuclearity is to dramatically enhance selectivity for comonomer enchainment in these copolymerizations.

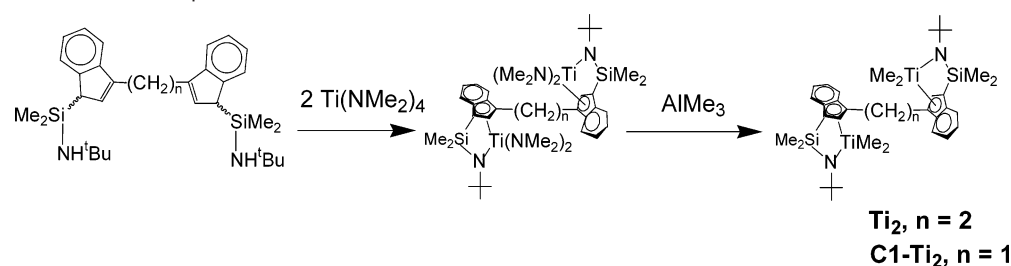
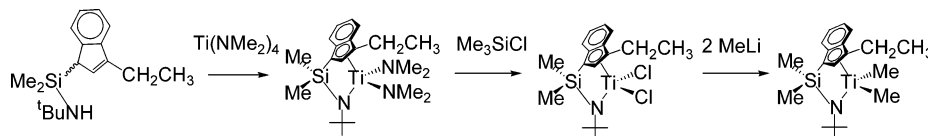
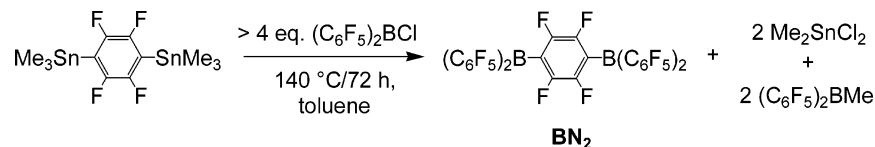
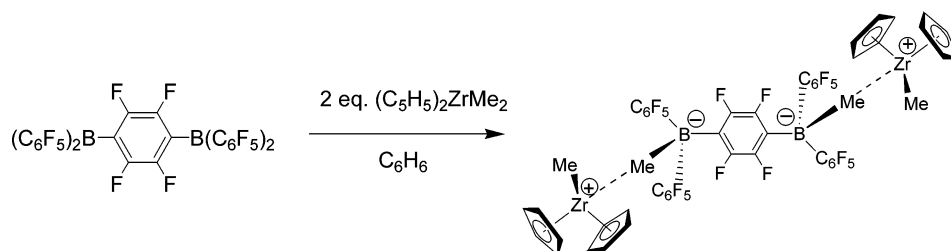
Results

The goal of this study was to investigate nuclearity effects for severely encumbered isoalkene enchainment in ethylene copolymerizations using the coordinatively “open” and highly reactive CGCTi (constrained geometry catalyst) core structures and to explore selectivity effects for isoalkene incorporation in polyethylene backbones arising from cooperative effects between proximate single-site catalytic centers. Thus, the new bimetallic constrained geometry catalysts (CGC), **Ti₂**, **C1–Ti₂**, the monometallic CGC complex, **Ti₁**, and the binuclear bisborane cocatalyst, 1,4-(C₆F₅)₂BC₆F₄B(C₆F₅)₂ (**BN₂**), were synthesized for this purpose. It will be seen that the effect of increasing catalyst and cocatalyst nuclearity is to significantly enhance sterically encumbered comonomer incorporation in the copolymerizations, producing new and unusual polyolefin copolymers.

I. Synthesis and Characterization of Bimetallic Metallocene Complexes, EBICGC(TiMe₂)₂ (Ti₂) and MBICGC(TiMe₂)₂ (C1–Ti₂).¹² The ligand (μ -CH₂CH₂-3,3') $\{1-(Me_2SiNH'Bu)indenyl\}_2$ (EBICGCH₂), synthesized according to the literature procedure,^{4f} consists of two diastereomers (*RR,SS*) and (*RS,SR*) in an approximate 1:1 ratio as indicated by ¹H and ¹³C NMR spectroscopy. Similar to the synthesis of the Zr analogue, bimetallic metallocene complex EBICGC(TiMe₂)₂ (**Ti₂**) was synthesized via the methodology outlined in Scheme 1. The first step is the synthesis of the bimetallic amido complex EBICGC[Ti(NMe₂)₂]₂ (**1**) via the protodeaminative reaction of the free (3,3'-CH₂CH₂) $\{1-Me_2SiNH'Bu\}ind_2$ ligand (EBICGCH₂) with Ti(NMe₂)₄ in refluxing toluene, with constant removal of the evolved HNMe₂ byproduct. The bimetallic product consists of two diastereomers (*RS,SR*) and (*SS,RR*) (1:1.3 or 1.3:1 ratio) as indicated by ¹H NMR spectroscopy. Both diastereomers have relatively low solubility in toluene and benzene and are almost completely insoluble in pentane. Attempts to isolate significant quantities of the pure diastereomers by fractional crystallization were unsuccessful. Bimetallic amido complex **1** was characterized by standard spectroscopic and analytical techniques, and one diastereomer (*RS,SR*) by X-ray diffraction (vide infra). Reaction of **1** with excess AlMe₃ at room temperature cleanly forms the bimetallic metallocene tetramethyl complex **Ti₂** (Scheme 1), which can be purified by repeated washing with pentane, and was characterized by conventional spectroscopic and analytical techniques. Both diastereomers (*RS,SR*) and (*SS,SR*)

- (8) (a) Takeuchi, D.; Anada, K.; Osakada, K. *Macromolecules* **2002**, *35*, 9628–9633. (b) Takeuchi, D.; Osakada, K. *Chem. Commun.* **2002**, 646–467. (c) Takeuchi, D.; Kim, S.; Osakada, K. *Angew. Chem., Int. Ed.* **2001**, *14*, 2685–2688.
- (9) (a) Kulshrestha, A. K.; Talapatra, S. In *Handbook of Polyolefins*; Vasile, C., Ed; Marcel Dekker: New York, 2000. (b) McKnight, A. L.; Waymouth, R. M. *Macromolecules* **1999**, *32*, 2816–2825. (c) Natori, I.; Imaizumi, K.; Yamagishi, H.; Kazunori, M. *J. Polym. Sci., Part B: Polym. Phys.* **1998**, *36*, 1657–1668. (d) Natori, I. *Macromolecules* **1997**, *30*, 3696–3697. (e) Cherdron, H.; Brekner, M.-J.; Osan, F. *Angew. Makromol. Chem.* **1994**, *223*, 121–133. (f) James, D. E. In *Encyclopedia of Polymer Science and Engineering*; Marks, H. F., Bikales, N. M., Overberger, C. G., Menges, G., Eds.; Wiley-Interscience: New York, 1985; Vol. 6.
- (10) (a) Zhao, J.; Hahn, S. F.; Hucul, D. A.; Meunier, D. M. *Macromolecules* **2001**, *34*, 1737–1741. (b) Hucul, D. A.; Hahn, S. F. *Adv. Mater.* **2000**, *12*, 1855–1858.
- (11) (a) Hahn, S. F.; Hillmyer, M. A. *Macromolecules* **2003**, *36*, 71–76. (b) Ness, J. S.; Brodil, J. C.; Bates, F. S.; Hahn, S. F.; Hucul, D. A.; Hillmyer, M. A. *Macromolecules* **2002**, *35*, 602–609. (c) Gehlsen, M. D.; Weimann, P. A.; Bates, F. S.; Mays, J. J. *Polym. Sci., Part B: Polym. Phys.* **1995**, *33*, 1527–1536. (d) Gehlsen, M.; Bates, F. S. *Macromolecules* **1993**, *26*, 4122–4127.

- (12) Detailed synthetic and characterization data can be found in the Supporting Information.

Scheme 1. Synthetic Routes to Complexes **Ti₂** and **C1-Ti₂****Scheme 2.** Synthetic Route to Complex **Ti₁****Scheme 3.** Synthetic Route to Complex **BN₂****Scheme 4.** Preparation of $[(C_5H_5)_2ZrMe^+]_2\{Me_2-1,4-C_6F_4[B(C_6F_5)_2]_2\}^{2-}$ 

RR) (1:1.3 or 1.3:1 ratio) are present in the product. The solubility of either diastereomer in toluene, benzene, and pentane is rather low, even at elevated temperatures. Furthermore, the complexes begin to decompose above 80 °C in solution, which also thwarts recrystallization.

Methylene-bridged bimetallic complex MBICGC(TiMe₂)₂ (**C1-Ti₂**) was similarly synthesized from the ligand (*μ*-CH₂-3,3')-[1-(Me₂SiNH*t*Bu)indenyl]₂ (MBICGCH₂; Scheme 2).^{4a} The synthetic conditions are similar to those outlined for the **Ti₂** synthesis above, except that longer reaction times are required in the metalation step, presumably due to the steric encumbrance.

II. Synthesis of [1-Me₂Si(3-ethylindenyl)(*t*BuN)]TiMe₂ (Ti₁**).** The monometallic metallocene complex [1-Me₂Si(3-ethylindenyl)(*t*BuN)]TiMe₂ (**Ti₁**) was synthesized as a mononuclear control for studies of binuclear cooperativity in ethylene polymerizations and copolymerizations. The ligand (1-Me₂SiNH*t*Bu)(3-ethyl)indene was synthesized according to the literature procedure.^{4f} The monometallic CGC complex [1-Me₂Si(3-ethylindenyl)(*t*BuN)]TiMe₂ (**Ti₁**) was synthesized via protodeaminative methodology similar to that for the monometallic zirconium complex [1-Me₂Si(3-ethylindenyl)(*t*BuN)]ZrMe₂ (**Zr₁**; Scheme 2). Thus, the monometallic Ti amido complex [1-Me₂Si(3-ethylindenyl)(*t*BuN)]Ti(NMe₂)₂ (**2**) was synthesized via reaction of the free (1-Me₂SiNH*t*Bu)(3-ethyl)indene ligand with Ti(NMe₂)₄ in refluxing toluene under constant removal of HNMe₂. The reaction of **2** with excess Me₃SiCl at room temperature then cleanly affords dichloro complex 1-Me₂Si(3-

ethylindenyl)(*t*BuN)TiCl₂, and subsequent reaction with MeLi affords metallocene dimethyl complex 1-Me₂Si(3-ethylindenyl)(*t*BuN)TiMe₂ (**Ti₁**). Complex **Ti₁** was characterized by standard spectroscopic and analytical techniques and by X-ray diffraction (vide infra).

III. Synthesis of Binuclear Bisborane Cocatalyst 1,4-(C₆F₅)₂BC₆F₄B(C₆F₅)₂ (BN₂**).** The synthesis of binuclear bisborane 1,4-(C₆F₅)₂BC₆F₄B(C₆F₅)₂ (**BN₂**) was accomplished by heating 1,4-C₆F₄(SnMe₃)₂ with 6.0 equiv of (C₆F₅)₂BCl in toluene for 72 h (Scheme 3). Alternatively (Method II), the neat reagents without solvent can be used to shorten the reaction time to 24 h.¹² As judged by ¹H and ¹⁹F NMR spectroscopy, alkyl/chloride exchange occurs initially to afford 2.0 equiv of (C₆F₅)₂BMe and 1,4-C₆F₄(SnMe₂Cl)₂; the latter then reacts with the additional (C₆F₅)₂BCl to yield 1,4-(C₆F₅)₂BC₆F₄B(C₆F₅)₂ (**BN₂**) and 2.0 equiv of Me₂SnCl₂ (Scheme 3). Purification of the crude reaction mixture is relatively straightforward; 1,4-(C₆F₅)₂BC₆F₄B(C₆F₅)₂ (**BN₂**) is insoluble in pentane, while (C₆F₅)₂BMe, Me₂SnCl₂, and the excess (C₆F₅)₂BCl are pentane-soluble and can be readily washed away.

IV. Synthesis of [(C₅H₅)₂ZrMe⁺]₂{Me₂-1,4-C₆F₄[B(C₆F₅)₂]₂}²⁻. Reaction of **BN₂** with 2.0 equiv of (C₅H₅)₂ZrMe₂ results in the clean, instantaneous formation of the bimetallic ion pair [(C₅H₅)₂ZrMe⁺]₂{Me₂-1,4-C₆F₄[B(C₆F₅)₂]₂}²⁻ (Scheme 4). This indicates that any intermediate abstraction product resulting from reaction of bisborane with 1.0 equiv of (C₅H₅)₂-ZrMe₂ is sufficiently Lewis acidic to abstract a methide anion

Table 1. Summary of the Crystal Structure Data for Complexes **1** and **Ti₁**

complex	1	Ti₁
formula	C ₄₀ H ₆₈ N ₆ Si ₂ Ti ₂	C ₁₉ H ₃₁ NSiTi
formula weight	784.98	349.44
crystal dimensions	0.50 × 0.45 × 0.35	0.11 × 0.16 × 0.21
crystal system	triclinic	monoclinic
<i>a</i> , Å	8.3171(2)	22.9273(14)
<i>b</i> , Å	9.8177(2)	12.1450(7)
<i>c</i> , Å	13.8667(4)	14.1744(8)
α, deg	83.5443(10)	90
β, deg	82.2403(11)	100.7690(10)
γ, deg	83.5394(8)	90
<i>V</i> , Å ³	1111.62(8)	3877.4(4)
space group	<i>P</i> $\bar{1}$	<i>C</i> 2/ <i>c</i>
<i>Z</i> value	2	8
<i>D</i> _{calc} , mg/m ³	1.173	1.197
temp, K	198(2)	153(2)
<i>μ</i> , cm ⁻¹	4.46	5.01
radiation	Mo Kα	Mo Kα
2θ range, deg	1.49 to 28.05	1.81 to 28.28
No. of parameters	241	323
intensities (unique, <i>R</i> _i)	4676, 0.0593	4652, 0.0282
<i>R</i>	0.1142	0.0534
<i>wR</i> ²	0.2631	0.1099

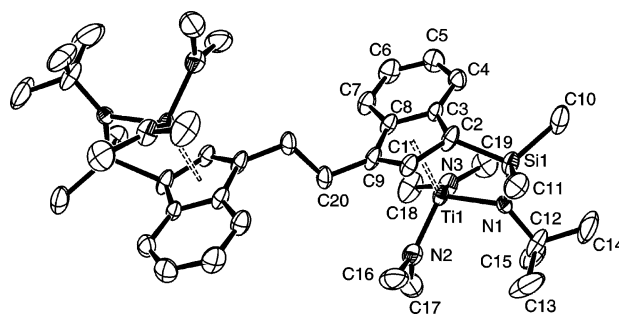
from a second neutral metallocene dialkyl. The displacements in the ¹⁹F chemical shifts of **BN₂** upon formation of [(C₅H₅)₂ZrMe⁺]₂[Me₂-1,4-C₆F₄[B(C₆F₅)₂]₂]²⁻ (i.e., upon bisanion formation) are similar to those observed for B(C₆F₅)₃,^{13e} with the exception of the ¹⁹F resonance arising from the central C₆F₄ ring of **BN₂**. This resonance is displaced 15 ppm upfield upon ion pair formation, relative to the more usual upfield perturbations of ca. 5 ppm observed for the B(C₆F₅)₂ for *ortho*-fluorine resonances,¹³ qualitatively indicating that a relatively large amount of electron density is transferred to the central C₆F₄ ring in the (C₅H₅)₂ZrMe⁺]₂[Me₂-1,4-C₆F₄[B(C₆F₅)₂]₂]²⁻ product.

Molecular Structures of the Complexes EBICGC[Ti(NMe₂)₂]₂ (Ti₁), [1-Me₂Si(3-Ethylindenyl)(ⁱBuN)]TiMe⁺MeB(C₆F₅)₃⁻, and [(C₅H₅)₂ZrMe⁺]₂[Me₂-1,4-C₆F₄[B(C₆F₅)₂]₂]²⁻:

A. Bimetallic Complex EBICGC[Ti(NMe₂)₂]₂ (1). A summary of crystal structure data for complex **1** is presented in Table 1, and selected bond distances and angles for **1** are summarized in Table 2. The crystal structure of complex **1** (Figure 1) reveals an inversion center with a CGCTi unit located on either side of the ethylenebis(indenyl) fragment and with the two π-coordinated indenyl rings in a diastereomeric relationship. As can be seen from Figure 1, the crystal consists of a single diastereomer (*SR*, *RS*). The sum of the bond angles around nitrogen atom N(1) is 358.8°, indicating that atoms Si(1), N(1), C(12), and Ti(1) are essentially coplanar, which is also true for the atoms surrounding dimethylamido atoms N(2) and N(3). Such coplanar structures suggest non-negligible π-bonding between the Ti and N atoms involving the N atom lone pair electrons.¹⁴ Nevertheless, the ⁱBuN–Ti bond (Ti(1)–N(1)) is 1.994(4) Å, substan-

Table 2. Selected Bond Distances (Å) and Angles (deg) for EBICGC[Ti(NMe₂)₂]₂ (**1**)

Bond Distances			
Ti(1)–N(1)	1.994(4)	Ti(1)–N(2)	1.940(4)
Ti(1)–N(3)	1.914(4)	Ti(1)–C(1)	2.395(4)
Ti(1)–C(2)	2.353(5)	Ti(1)–C(3)	2.516(5)
Ti(1)–C(8)	2.599(5)	Ti(1)–C(9)	2.512(5)
N(1)–C(12)	1.497(6)	N(2)–C(16)	1.465(7)
Si(1)–C(2)	1.878(5)	Si(1)–N(1)	1.732(4)
Angles			
N(3)–Ti(1)–N(2)	102.0(2)	N(3)–Ti(1)–N(1)	104.7(2)
N(2)–Ti(1)–N(1)	105.9(2)	N(1)–Si(1)–C(2)	94.6(2)
N(1)–Si(1)–C(11)	117.1(14)	C(2)–Si(1)–C(11)	108.4(2)
N(1)–Si(1)–C(10)	115.5(3)	C(12)–N(1)–Si(1)	126.5(3)
C(12)–N(1)–Ti(1)	128.8(3)	Si(1)–N(1)–Ti(1)	103.5(2)
C(16)–N(2)–C(17)	109.1(5)	C(16)–N(2)–Ti(1)	124.8(4)
C(17)–N(2)–Ti(1)	125.8(4)	C(18)–N(3)–C(19)	110.9(5)
C(18)–N(3)–Ti(1)	119.5(4)	C(19)–N(3)–Ti(1)	127.6(4)
C(1)–C(2)–C(3)	105.4(2)	C(1)–C(2)–Si(1)	119.6(3)
C(3)–C(2)–Si(1)	126.5(3)	C(1)–C(9)–C(8)	106.5(4)
C(1)–C(9)–C(20)	127.7(4)	C(8)–C(9)–C(20)	125.1(4)

**Figure 1.** The molecular structure and atom numbering scheme for the binuclear complex EBICGC[Ti(NMe₂)₂]₂ (**1**). Thermal ellipsoids are drawn at the 50% probability level. A single enantiomer is shown.

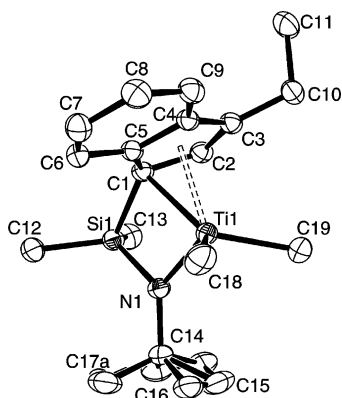
tially longer than the Ti–NMe₂ bonds (Ti(1)–N(2) = 1.940(4) Å, Ti(1)–N(3) = 1.914(4) Å), likely owing to steric constraints in addition to the decreased basicity¹⁵ of the (Me₂Si)ⁱBuN moiety. The sum of bond angles around ring carbon atom C(2) is 351.5°, indicating that the C(2)–Si(1) bond vector is displaced appreciably from the ring plane because of the constrained geometry. As expected, the Me₂Si < bridge forces the ind plane to tilt, increasing the ring centroid–Ti–N angle and making the structure more open—the N(1)–Ti(1)–centroid(1) angle is 106.58(6)°. The carbon atoms of the Cp ring do not exhibit equal bonding distances to the Ti center. The average bond lengths of Ti–C1/Ti–C2 and Ti–C3/Ti–C8/Ti–C9 are 2.374 and 2.542 Å, respectively. The difference Δ (Ti–C3/Ti–C8/Ti–C9) – (Ti–C1/Ti–C2) is 0.168 Å, 0.037 Å greater than that value found for the more symmetrical Cp ligand in [(η⁵-C₅Me₄)SiMe₂(*N-t*-Bu)]TiCl₂, which is 2.436 – 2.305 = 0.131 Å,^{14f} indicating a substantially more “slipped” coordination of the Cp ligand in **1**.

(13) (a) Song, F.; Lancaster, S. J.; Cannon, R. D.; Schormann, M.; Humphrey, S. M.; Zuccaccia, C.; Macchioni, A.; Bochmann, M. *Organometallics* **2005**, *24*, 1315–1328. (b) Hannig, F.; Fröhlich, R.; Bergander, K.; Erker, G.; Petersen, J. L. *Organometallics* **2004**, *23*, 4495–4502. (c) Beck, S.; Lieber, S.; Schaper, F.; Geyer, A.; Brintzinger, H. H. *J. Am. Chem. Soc.* **2001**, *123*, 1483–1489. (d) Chase, P. A.; Piers, W. E.; Patrick, B. O. *J. Am. Chem. Soc.* **2000**, *122*, 12911–12912. (e) Yang, X.; Stern, C. L.; Marks, T. J. *J. Am. Chem. Soc.* **1994**, *116*, 10015–10031. (f) Yang, X.; Stern, C. L.; Marks, T. J. *J. Am. Chem. Soc.* **1991**, *113*, 3623–2625. (g) Bochmann, M.; Lancaster, S. J.; Hursthouse, M. B.; Abdul Malik, K. M. *Organometallics* **1994**, *13*, 2235–2243. (h) Stahl, N. G.; Salata, M. R.; Marks, T. J. *J. Am. Chem. Soc.* **2005**, *127*, 10898–10909.

(14) (a) Christopher, J. N.; Jordan, R. F.; Petersen, J. L.; Young, V. G., Jr. *Organometallics* **1997**, *16*, 3044–3050. (b) Diamond, G. M.; Jordan, R. F.; Petersen, J. L. *Organometallics* **1996**, *15*, 4030–4037. (c) Christopher, J. N.; Diamond, G. M.; Jordan, R. F.; Petersen, J. L. *Organometallics* **1996**, *15*, 4038–4044. (d) Diamond, G. M.; Jordan, R. F.; Petersen, J. L. *Organometallics* **1996**, *15*, 4045–4053. (e) Diamond, G. M.; Jordan, R. F.; Petersen, J. L. *J. Am. Chem. Soc.* **1996**, *118*, 8024–8033. (f) Carpenetti, D. W.; Kloppenburg, L.; Kupec, J. T.; Petersen, J. L. *Organometallics* **1996**, *15*, 1572–1581. (g) Lappert, M. F.; Power, P. P.; Sanger, A. R.; Srivastava, R. C. *Metal and Metalloid Amides*; Ellis Horwood: Chichester, West Sussex, U.K., 1980; pp 500–502. (h) Bradley, D. C.; Chisholm, M. H. *Acc. Chem. Res.* **1976**, *9*, 273–280. (15) Barlos, K.; Huebler, G.; Noth, H.; Wanninger, P.; Wiberg, N.; Wrackmeyer, B. *J. Magn. Reson.* **1978**, *31*, 363–376.

Table 3. Selected Bond Distances (Å) and Angles (deg) for **Ti₁**

Bond Distances			
Ti(1)–N(1)	1.9300(15)	Ti(1)–C(19)	2.110(2)
Ti(1)–C(18)	2.102(2)	Ti(1)–C(2)	2.3430(17)
Ti(1)–C(5)	2.4120(17)	Ti(1)–C(1)	2.2869(16)
Ti(1)–C(4)	2.5428(17)	Ti(1)–C(3)	2.4940(17)
Si(1)–N(1)	1.7503(15)	Si(1)–C(13)	1.859(2)
Si(1)–C(12)	1.8640(17)	Si(1)–C(2)	1.869(2)
N(1)–C(14)	1.493(2)		
Angles			
N(1)–Ti(1)–C(19)	108.85(8)	N(1)–Ti(1)–C(18)	109.15(9)
C(19)–Ti(1)–C(18)	101.58(9)	N(1)–Si(1)–C(13)	115.69(9)
N(1)–Si(1)–C(12)	115.72(9)	C(13)–Si(1)–C(12)	108.27(11)
N(1)–Si(1)–C(1)	93.64(7)	C(14)–N(1)–Si(1)	126.64(12)
C(14)–N(1)–Ti(1)	130.84(12)	Si(1)–N(1)–Ti(1)	102.51(7)
C(2)–C(1)–C(5)	104.65(14)	C(2)–C(1)–Si(1)	120.21(13)
C(5)–C(1)–Si(1)	125.65(12)	C(2)–C(3)–C(4)	107.00(15)
C(2)–C(3)–C(10)	126.97(16)	C(4)–C(3)–C(10)	125.56(16)

**Figure 2.** The molecular structure and atom numbering scheme for the mononuclear complex (3-CH₃C₂H-indenyl)[1-SiMe₂(^tBuN)]TiMe₂ (**Ti₁**). Thermal ellipsoids are drawn at the 50% probability level. A single enantiomer is shown.

B. Monometallic Complex **Ti₁.** A summary of crystal structure data for dimethyl complex **Ti₁** is compiled in Table 1, and selected bond distances and angles for **Ti₁** are summarized in Table 3. The solid-state structure of monometallic **Ti₁** is illustrated in Figure 2, and it can be seen that the three methyl groups on the *tert*-butyl amido group are disordered. As expected, the metrical parameters in Table 4 suggest that the Me₂Si < bridge again forces the ind plane to tilt, rendering the structure more open; the N(1)–Ti(1)–centroid(1) is 109.55(6)°, comparable to the N(1)–Ti(1)–centroid(1) value in similar CGCTi– structures: 105.5° in [(η⁵-C₅H₄)SiMe₂(^tBuN)]Ti(NMe₂)₂;^{14f} 108.3° in [(η⁵-C₉H₅-2-NMe₂)SiMe₂(^tBuN)]TiCl₂;^{16a} 103.85° in [(η⁵-C₅Me₄)SiMe₂(η¹-NNMe₂)]Ti(NMe₂)₂;^{16b} 107.3° in [(η⁵:η¹-C₅H₄CMe₂)SiMe₂(^tBuN)]TiCl₂;^{16c} 106.3° in (+)-(R)-[η⁵:η¹-(Ind)SiMe₂-(S)-NCHMePh]TiCl₂.^{16d} Similar to bimetallic complex **1**, the sum of the bond angles around bridge-connected nitrogen atom N(1) in **Ti₁** is close to 360°, indicating the atoms around N(1) are essentially coplanar, again suggesting strong Ti–N bonding,¹⁴ presumably involving π-donation.^{14g,h} Compared to bimetallic dimethylamido complex **1**, both the Ti–N(1) and Ti–C(ring) bond lengths in dimethyl **Ti₁** are signifi-

Table 4. Summary of the Crystal Structure Data for Complexes **2** and **3**

complex	2	3
formula	C ₄₄ H ₃₉ BF ₁₅ NSiTi	C ₇₆ H ₄₂ B ₂ F ₂₄ Zr ₂
formula weight	953.56	1615.19
crystal dimensions	0.12 × 0.17 × 0.22	0.28 × 0.26 × 0.010
crystal system	triclinic	triclinic
<i>a</i> , Å	11.0774(8)	11.40(1)
<i>b</i> , Å	12.8788(9)	11.52(1)
<i>c</i> , Å	16.3857(12)	15.24(1)
α, deg	90.2610(10)	67.97(4)
β, deg	97.9910(10)	88.4(1)
γ, deg	110.6800(10)	66.31(4)
<i>V</i> , Å ³	2162.2(3)	1682(2)
space group	P $\bar{1}$	P $\bar{1}$
<i>Z</i> value	2	1
<i>D</i> _{calc} , mg/m ³	1.465	1.595
temp, K	153(2)	153(2)
μ, cm ^{−1}	3.24	4.21
radiation	Mo Kα	Mo Kα
2θ range, deg	1.26 to 28.30	1.46 to 22.97
No. of parameters	243	279
intensities (unique, <i>R_i</i>)	10009, 0.0379	2922, 0.0539
<i>R</i>	0.0794	0.0842
<i>wR</i> ²	0.1556	

Table 5. Selected Bond Distances (Å) and Angles (deg) for **2**

Bond Distances			
Ti(1)–N(1)	1.898(2)	Ti(1)–C(19)	2.320(2)
Ti(1)–C(18)	2.090(3)	Ti(1)–C(1)	2.246(2)
Ti(1)–C(5)	2.333(2)	Ti(1)–C(2)	2.320(2)
Ti(1)–C(4)	2.535(2)	Ti(1)–C(3)	2.484(2)
Si(1)–N(1)	1.762(2)	Si(1)–C(13)	1.855(3)
Si(1)–C(12)	1.855(3)	Si(1)–C(1)	1.861(2)
N(1)–C(14)	1.503(3)	C(19)–B(1)	1.675(3)
B(1)–C(20)	1.650(4)	B(1)–C(26)	1.639(4)
B(1)–C(32)	1.656(4)	C(32)–C(37)	1.387(3)
Angles			
N(1)–Ti(1)–C(18)	104.47(11)	N(1)–Ti(1)–C(1)	77.79(8)
C(18)–Ti(1)–C(1)	125.73(10)	N(1)–Ti(1)–C(19)	109.58(9)
C(18)–Ti(1)–C(19)	100.50(10)	N(1)–Si(1)–C(13)	114.40(13)
N(1)–Si(1)–C(12)	114.09(13)	C(13)–Si(1)–C(12)	111.49(15)
N(1)–Si(1)–C(1)	92.40(10)	C(13)–Si(1)–C(1)	110.46(12)
C(12)–Si(1)–C(1)	112.65(13)	C(14)–N(1)–Si(1)	125.08(16)
C(14)–N(1)–Ti(1)	132.56(16)	Si(1)–N(1)–Ti(1)	102.22(10)
B(1)–C(19)–Ti(1)	169.04(18)	C(26)–B(1)–C(20)	113.8(2)
C(26)–B(1)–C(32)	104.8(2)	C(20)–B(1)–C(32)	113.8(2)
C(26)–B(1)–C(19)	112.5(2)	C(20)–B(1)–C(19)	103.5(2)
C(32)–B(1)–C(19)	108.5(2)	C(37)–C(32)–B(1)	127.2(2)

cantly shorter. Thus, Ti(1)–N(1) is 1.994(4) Å in **1** and 1.9300(15) Å in **Ti₁**; Ti(1)–C(9) is 2.512(4) Å in **1**, and the corresponding Ti(1)–C(3) contact in **Ti₁** is 2.4940(17) Å. The expanded bond distances in **1** are no doubt because the Ti center is more electron-rich, presumably due to Ti–N bonding involving the dimethylamido nitrogen lone pairs.

C. Activated Ti Complex [1-Me₂Si(3-Ethylindenyl)(^tBuN)]-TiMe⁺MeB(C₆F₅)₃[−] (2**).** A summary of crystal structure data for complex **2** is given in Table 4; selected bond distances and angles for **2** are summarized in Table 5, and the molecular structure is shown in Figure 3. The Ti–Me(terminal) distance (2.090(3) Å) is 0.01–0.02 Å shorter than the Ti–Me distances in neutral **Ti₁** (2.102(2) and 2.1100(2) Å) due to the increased electrophilic character, while it is 0.230 Å shorter than the Ti–Me(bridging) separation (2.320(2) Å), reflecting the largely ionic character of the ion pair interaction.^{13,17,18} The metrical parameters in **2** are similar to those in (η⁵-Me₄C₅)Me₂Si(^tBuN)TiMe⁺MeB(C₆F₅)₃[−], except the Ti–Me(bridging) distance:¹⁹ it is 2.320(2) Å in **2**, while 2.364(2) Å in Me₂Si(η⁵-Me₄C₅)(^tBuN)-

(16) (a) Klosin, J.; Kruper, W. J., Jr.; Nickias, P. N.; Roof, G. R.; De Waele, P.; Abboud, K. A. *Organometallics* **2001**, *20*, 2663–2665. (b) Park, J. T.; Yoon, S. C.; Bae, B.-J.; Seo, W. S.; Suh, I.-H.; Han, T. K.; Park, J. R. *Organometallics* **2000**, *19*, 1269–1276. (c) Feng, S.; Klosin, J.; Kruper, W. J., Jr.; McAdon, M. H.; Neithamer, D. R.; Nickias, P. N.; Patton, J. T.; Wilson, D. R.; Abboud, K. A.; Stern, C. L. *Organometallics* **1999**, *18*, 1159–1167. (d) McKnight, A. L.; Masood, M. A.; Waymouth, R. M.; Straus, D. A. *Organometallics* **1997**, *16*, 2879–2885.

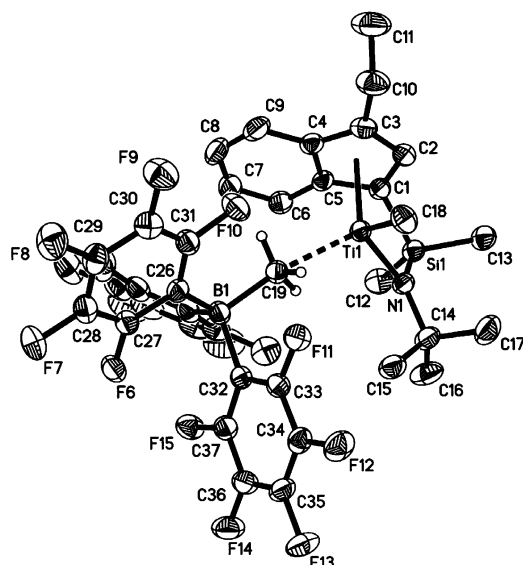


Figure 3. The molecular structure and atom numbering scheme for the mononuclear ion pair [1-Me₂Si(3-ethylindenyl)(tBuN)]TiMe⁺MeB(C₆F₅)₃⁻ (**2**). Thermal ellipsoids are drawn at the 50% probability level.

TiMe⁺MeB(C₆F₅)₃⁻. The difference in the Ti–Me(bridging) separation probably reflects differences in steric interactions between the MeB(C₆F₅)₃⁻ anion and the various substituted Cp ligands. Additionally, the Ti–N and Ti–C(Cp ring) bond distances in **2** are substantially shorter than those in neutral **Ti1**: Ti(1)–N(1) = 1.898(2) Å in **2** versus 1.930(2) Å in **Ti1**; Ti(1)–C(1) is 2.246(2) Å in **2** versus 2.287(2) Å in **Ti1**, which is doubtless due to the increased electrophilic character of cationic center. The B(1)–C(19)–Ti(1) bond angle = 169.04(18)° indicates that the cation–anion bridge is essentially linear. The B–Me distance (1.675(3) Å) in **2** is typical of a B–Me(bridging) bond lengths for B(C₆F₅)₃-derived ion pairs.¹³

D. Activated Bimetallic Complex [(C₅H₅)₂ZrMe⁺]₂{Me₂-1,4-C₆F₄[B(C₆F₅)₂]₂}²⁻ (3**).** A summary of crystal structure data for complex **3** is given in Table 4, and selected bond distances and angles for **3** are collected in Table 6. The crystal structure is shown in Figure 4. The two zirconocenium cations are centrosymmetrically disposed on opposite sides of the arene plane, presumably reflecting repulsive steric and electrostatic interactions. The structural features about the zirconocenium fragments are similar to those in mononuclear analogues, such as Cp₂ZrMe⁺MeB(C₆F₅)₃⁻ (**I**)²⁰ and (C₅R₅)₂ZrMe⁺MeB(C₆F₅)₃⁻ complexes^{13e} [C₅R₅ = η⁵-1,2-Me₂C₅H₃ (**II**), η⁵-1,3-(SiMe₃)₂C₅H₃ (**III**), and η⁵-C₅Me₅ (**IV**)]. The Zr–Me(terminal) distance (2.26(1)Å) is 0.26 Å shorter than the Zr–Me(bridging) separation (2.52(1) Å). The Zr–C–B angle (161.3°) is somewhat smaller than that in **I** (169.1°). The increased bending of the Zr–C–B angle in complex **3** is likely due to the greater steric bulk of the Me₂-1,4-C₆F₄[B(C₆F₅)₂]₂²⁻ dianion versus the MeB(C₆F₅)₃⁻ monoanion. The Zr–Me(bridging) distance in **3**

Table 6. Selected Bond Distances (Å) and Angles (deg) for **3**

Bond Distances			
Zr(1)–C(1)	2.51(1)	Zr(1)–C(6)	2.54(1)
Zr(1)–C(11)	2.26(1)	Zr(1)–C(12)	2.52(1)
F(1)–C(14)	1.36(1)	F(6)–C(20)	1.37(2)
F(11)–C(26)	1.37(1)	C(1)–C(2)	1.41(2)
C(1)–C(2)	1.41(2)	C(9)–C(10)	1.40(2)
C(13)–C(14)	1.35(2)	C(19)–C(20)	1.36(2)
C(25)–C(26)	1.39(2)	C(12)–B(1)	1.64(2)
C(13)–B(1)	1.70(2)	C(19)–B(1)	1.67(2)
C(25)–B(1)	1.65(2)		
Angles			
C(1)–Zr(1)–C(8)	98.8(5)	C(1)–Zr(1)–C(12)	88.3(5)
C(11)–Zr(1)–C(12)	92.6(5)	Zr(1)–C(12)–B(1)	161.3(9)
F(1)–C(14)–C(13)	123(1)	F(1)–C(14)–C(15)	112(1)
C(3)–C(4)–C(5)	108(1)	C(13)–C(14)–C(15)	125(1)
C(12)–B(1)–C(13)	113(1)	C(12)–B(1)–C(19)	114(1)
C(12)–B(1)–C(25)	104(1)	C(13)–B(1)–C(19)	102(1)
C(13)–B(1)–C(25)	112(1)	C(19)–B(1)–C(25)	112(1)

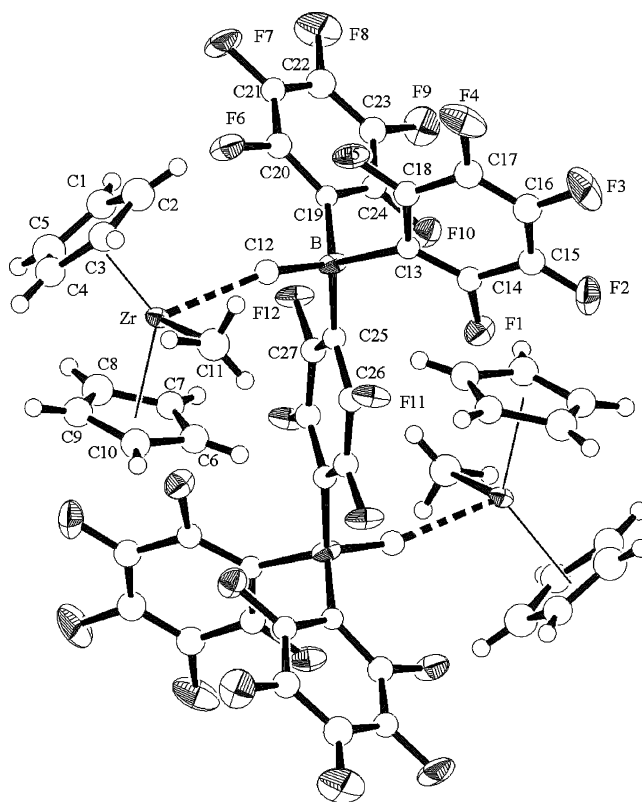
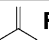
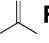
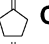
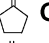
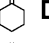
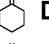
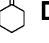
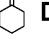
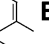
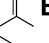
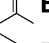
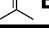


Figure 4. The molecular structure and atom numbering scheme for [(C₅H₅)₂ZrMe⁺]₂{Me₂-1,4-C₆F₄[B(C₆F₅)₂]₂}²⁻ (**3**). Thermal ellipsoids are drawn at the 50% probability level.

(2.52(1) Å) is similar to those in **I** (2.556(2) Å) and in **II** (2.549–(3) Å), but shorter than those in **III** and **IV** (2.625(5) and 2.640–(7) Å, respectively). Similarly, the Zr–C(Cp) distances in **3** are similar to those in **I**, but slightly shorter than those in **II–IV**. The shorter Zr–Me and Zr–C(Cp) distances in **3** likely reflect the reduced steric requirements of C₅H₅⁻ versus substituted Cp⁻ ligands. The influence of the charge on the structure of the metallocene unit of **3** can be assessed by comparison of the structures of **3** and the neutral precursor Cp₂ZrMe₂ (**V**). Due to the increased electrophilic character of **3**, the Zr–Me(terminal) contact in **3** (2.26(1) Å) is presumably shorter than the corresponding distance in **V** (2.277(5) Å). The metrical parameters for the Me₂-1,4-C₆F₄[B(C₆F₅)₂]₂²⁻ dianion are similar to those found for the MeB(C₆F₅)₃⁻ anions.¹³

- (17) (a) Zuccaccia, C.; Stahl, N. G.; Macchioni, A.; Chen, M.-C.; Roberts, J. A.; Marks, T. J. *J. Am. Chem. Soc.* **2004**, *126*, 1448–1464. (c) Beswick, C. L.; Marks, T. J. *J. Am. Chem. Soc.* **2000**, *122*, 10358–10370. (d) Deck, P. A.; Beswick, C. L.; Marks, T. J. *J. Am. Chem. Soc.* **1998**, *120*, 1772–1784.
- (18) (a) Lanza, G.; Fragala, I. L.; Marks, T. J. *Organometallics* **2002**, *21*, 5594–5612. (b) Lanza, G.; Fragala, I. L.; Marks, T. J. *Organometallics* **2001**, *20*, 4006–4017. (c) Lanza, G.; Fragala, I. L.; Marks, T. J. *J. Am. Chem. Soc.* **2000**, *122*, 12764–12777.
- (19) Fu, P.; Marks, T. J. Unpublished results.
- (20) Guzei, I. A.; Stockland, R. A.; Jordan, R. F. *Acta Crystallogr.* **2000**, *C56*, 635–636.

Table 7. Ethylene + Isoalkene Copolymerization Results for Catalysts **Ti₂** and **Ti₁** with Cocatalysts **BN₂** and **BN^a**

Entry	Catalyst	Cocatalyst	Comonomer	Comonomer conc. (M)	μ mol of catalyst	Reaction time[<i>min</i>]	Polymer yield (g)	Activity(10^5) ^b	$10^{-3} M_w$ ^c	M_w/M_n ^c	Comonomer incorporation% ^d
1	Ti₁	BN	 F	1.2	10	5	0.80	9.6	577	2.1	3.1
2	Ti₂	BN₂	 F	1.2	5	5	0.47	2.8	168	3.6	15.2
3	Ti₁	BN	 C	1.6	10	5	0.67	8.0	503	2.4	8.3
4	Ti₂	BN₂	 C	1.6	5	5	0.49	5.9	186	2.3	20.4
5	Ti₁	BN	 D	1.4	10	4	0.87	13.0	475	1.8	3.3
6	Ti₂	BN₂	 D	1.4	5	6	0.35	3.5	369	2.8	8.3
7	Ti₁	BN	 D	Neat	10	8	0.64	4.8	320	2.2	6.8
8	Ti₂	BN₂	 D	Neat	5	8	0.37	2.8	297	2.4	15.9
9	Ti₁	BN	 E	2.7	10	5	0.61	7.3	769	2.9	1.1
10	Ti₂	BN₂	 E	2.7	5	5	0.47	5.6	503	1.9	2.5
11	Ti₁	BN	 E	Neat	10	10	0.73	4.4	486	2.1	3.2
12	Ti₂	BN₂	 E	Neat	5	10	0.65	3.9	456	1.8	7.3

^a Polymerizations carried out on high vacuum line at 24 °C under 1.0 atm ethylene pressure. ^b Gram polymer/[(mol cationic metallocene)·atm·h]. ^c From GPC versus polystyrene standards. ^d Mole percentage, calculated from ¹³C NMR spectra.²²

Methylenecycloalkane Homopolymerization Studies. Before attempting copolymerizations, the homopolymerizations of methylenecycloalkanes **C** and **D** were surveyed with catalysts **Ti₁** + **BN₁** and **Ti₂** + **BN₂**. In both cases, negligible yields of homopolymers are obtained on quenching the reaction mixture with MeOH. Only isomerization products **I** and **J** are detected. The sterical hindrance of the comonomer doubtless renders multiple enchainment sluggish.

Ethylene Copolymerization Studies. With the coordinatively open and reactive CGCTi catalysts, sterically hindered **C** and **D** are successfully incorporated into polyethylene backbones in a ring-unopened regiochemistry as will be discussed below. More interestingly, the severely sterically hindered monomer, 1,1,2-trisubstituted monomer **E**, also undergoes copolymerization with ethylene, albeit with formation of an unusual alternative microstructure (see below). For all of these encumbered comonomers, it will be seen that the binuclear catalysts/cocatalysts significantly enhance the comonomer enchainment selectivity versus the mononuclear analogues under identical reaction conditions. Similarly, as in the isobutene case reported previously,^{4d} CGCZr catalysts (**Zr₁** or **Zr₂**) in combination with any of the aforementioned cocatalysts introduce negligible quantities of methylenecycloalkane comonomers into the polyethylene products.

When olefins **C** and **D** are used as ethylene comonomers, the CGCTi catalysts cleanly incorporate the hindered comonomers in a ring-unopened regiochemistry to yield copolymers **K** and **L**, respectively (see Table 7 for data summary).²¹ To our knowledge, this is the first report of the formation of ethylene + methylenecyclopentane and ethylene + methylenecyclohex-

ane copolymers via coordination polymerization. Figure 5A shows the ¹³C NMR spectrum of the ethylene + **C** copolymer (Table 7, entry 3). Assignments have been made by comparison to the reported spectrum of an ethylene + **F** copolymer,^{4d} model compound 1,1-dimethylcyclopentane,^{22a} and from DEPT results (Figure 5B). The disappearance of peaks with chemical shifts in the $\delta \sim 45\text{--}46$ ppm region in the 45° DEPT spectrum (Figure 5B) indicates that they are quaternary carbons, with all others carbons being secondary. Thus resonances a, a', and b can be assigned as quaternary carbons joining cyclopentane ring and polymer backbone (depending on the number of ethylene units enchainment between the incorporated cyclopentanes, the chemical shifts of the different quaternary carbons vary slightly: peak b, having a single ethylene unit between two rings, a', having two ethylene units between the adjacent two rings, a, having three or more ethylene units between the two rings^{22c}). Carbons along the polyethylene chain adjacent to the quaternary carbons (peaks e, f, and g are assigned to the microstructures of enchainment cyclopentanes separated by two or more ethylene units; c and d are assigned to the microstructures of enchainment cyclopentanes separated by a single ethylene unit) have chemical shifts similar to those in the corresponding ethylene + isobutene copolymer chains^{4d} and can be assigned accordingly. Carbon resonances within the cyclopentane ring are assigned based on the model compound 1,1-dimethylcyclopentane;^{22a} peak j has an almost identical chemical shift to the carbon at the same position in the model compound, while the chemical shifts of resonances h and i are shifted ~ 3 ppm to high field, presumably reflecting the different influence of methyl versus polyethylene substituents. The ¹³C NMR data reveal that most of the enchainment methylenecyclopentane moieties are separated either by a single

(21) (a) $B(C_6F_5)_3$ does not initiate cationic methylenecycloalkane polymerization in toluene,^{21c} and the present copolymerizations with ethylene are inconsistent with a cationic pathway.^{21b,c} (b) Baird, M. C. *Chem. Rev.* **2000**, *100*, 1471–1478 and references therein. (c) Barsan, F.; Karam, A. R.; Parent, M. A.; Baird, M. C. *Macromolecules* **1998**, *31*, 8439–8447.

(22) (a) Breitmaier, E.; Voelter, W. *Carbon-13 NMR Spectroscopy*; VCH Publishers: Weinheim, Germany, 1987. (b) Spectral Database for Organic Compounds, SDBS. (c) The assignment is based on relative intensity changes of these peaks at different incorporation levels.

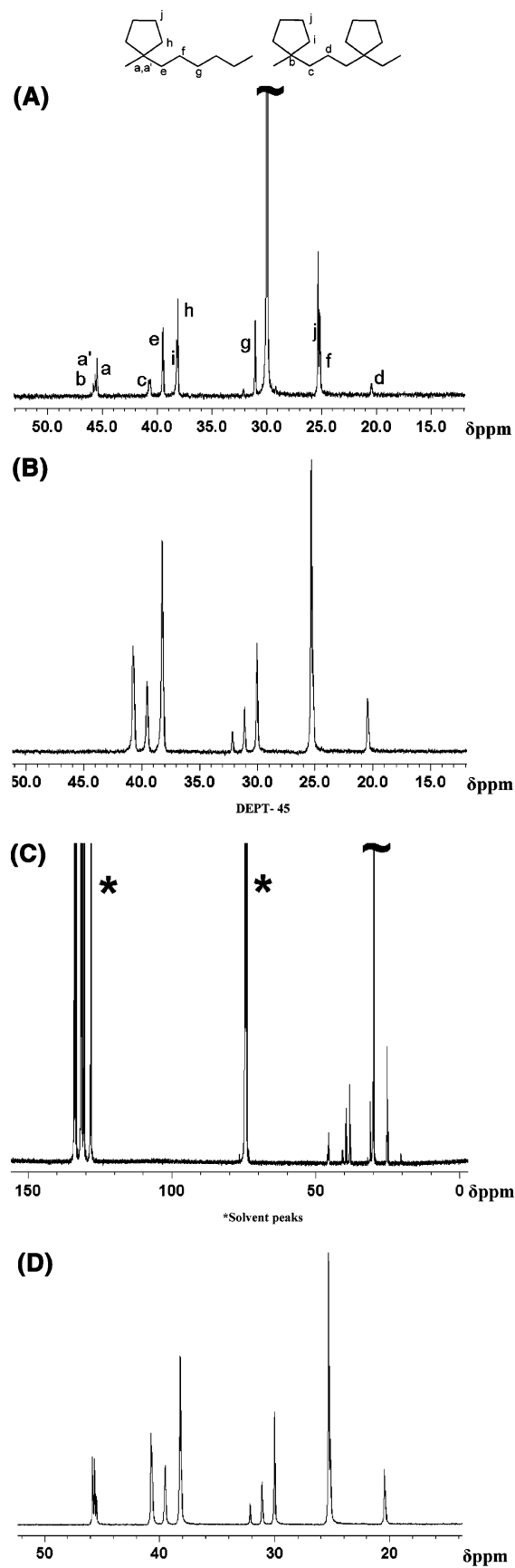


Figure 5. ^{13}C NMR spectra (100 MHz, $\text{C}_2\text{D}_2\text{Cl}_4$, 120 °C) of ethylene + methylenecyclopentane copolymers showing spectral assignments: (A) sample of Table 7, entry 3; (B) sample of Table 8, entry 6, DEPT spectrum; (C) Table 7, sample of entry 3, full spectrum; (D) sample of Table 8, entry 6.

ethylene unit or by two or more ethylene units, and there are no detectable microstructures with adjacent comonomer units, even under neat comonomer polymerization conditions (Table 8, entries 5 and 6). Note that in the spectrum of Figure 5C there are no features in the olefinic region, confirming the predominance of the ring-unopened enchainment pathway (ring-unopened structure **G** and **H**). Figure 5D shows the ^{13}C spectrum of the copolymer derived from copolymerization of ethylene + neat **C** (without toluene as the polymerization solvent; Table 8, entry 6), in which the comonomer incorporation level is so great that the resonances of the $-\text{CH}_2\text{CH}_2-$ segments are greatly diminished. Note that the percentage of the microstructure consisting of enchainment methylenecyclopentane units separated by a single ethylene unit in the copolymer increases correspondingly. Figure 6 shows the ^{13}C spectrum of the ethylene + **D** copolymer (Table 7, entry 7). Combined with the spectral information from the DEPT spectrum (Figure 6B), the ethylene + **E** copolymer,^{4d} and the model compound 1,1-dimethylcyclohexane,^{22a} all the peaks can be assigned analogously to the ethylene + **C** case.

To further increase the comonomer steric hindrance, 1,1,2-trisubstituted olefin **E** was also investigated in ethylene copolymerization experiments. The ^{13}C spectrum of the copolymer reveals a unique microstructure assigned to **M** (Table 7, entry 12), as shown in Figure 7. From the microstructural information provided by the DEPT spectrum (Figure 7B), the ethylene + isobutene copolymer,^{4d} and the model compound 3-ethyl-3-methylheptane,^{22b} all resonances can be assigned using the same arguments as for the other copolymers above.

Table 7 summarizes data for ethylene copolymerizations with isoalkenes **C–F** mediated by the various catalyst/cocatalyst combinations. The copolymer product molecular weight and polymerization activities decrease moderately with increasing catalyst/cocatalyst nuclearity or increasing comonomer concentration. The polymer polydispersities are around 2.0, which is typical for single-site polymerizations. The comonomer consumed during the copolymerization was typically $\sim 5\%$ of the total comonomer employed, thus maintaining the comonomer concentration essentially constant during the course of the polymerization. It can be seen from the incorporation levels compiled in Table 7 that the comonomer reactivity ordering for constant catalyst is $\text{C} > \text{D} \sim \text{F} \gg \text{E}$. This ordering largely parallels increasing monomer steric hindrance. While **C**, **D**, and **E** are in the same general range of reactivity, **E** is by far the least reactive among all comonomers investigated, presumably reflecting the pronounced steric encumbrance engendered by trisubstitution of the double bond and resulting in a different copolymerization pathway than traversed by the other three comonomers (see Discussion below).

Regarding nuclearity effects, it is found that under identical reaction conditions the $\text{Ti}_2 + \text{BN}_2$ catalyst incorporates ~ 2.5 times more **C**, ~ 2.5 times more **D**, ~ 2.3 times more **E**, and ~ 5 times more **F** than the mononuclear $\text{Ti}_1 + \text{BN}$ analogue. Table 8 summarizes the ethylene + **C** copolymerization results achieved by different catalysts under a variety of polymerization conditions. It can be seen that at higher comonomer incorporation levels, the binuclear enhancement effects on incorporation are diminished. Thus, Table 8 entry 4 versus 1 indicates that the binuclear catalyst/cocatalyst achieves ~ 2.5 times greater comonomer incorporation selectivity than the mononuclear

Table 8. Ethylene + Methylene-cyclopentane Copolymerization Results for Catalysts **Ti₂**, **C1–Ti₂**, and **Ti₁** with Cocatalysts **BN₂** and **BN^a**

entry	catalyst	cocatalyst	comonomer concentrated (M)	μ mol of catalyst	reaction time (min)	polymer yield (g)	activity (10 ⁵) ^b	10 ⁻³ M _w ^c	M _w /M _n ^c	comonomer incorporation (%) ^d	T _g (°C)
1	Ti₁	BN	1.6	10	5	0.67	8.0	503	2.4	8.3	-33.4
2	Ti₂	BN	1.6	5	5	0.61	7.3	342	2.1	13.3	-27.8
3	Ti₁	BN₂	1.6	10	5	0.55	6.6	285	1.9	14.8	-27.0
4	Ti₂	BN₂	1.6	5	5	0.49	5.9	186	2.3	20.4	-25.3
5	Ti₁	BN	neat	10	8	0.57	4.3	203	2.0	23.2	-21.7
6	Ti₂	BN₂	neat	5	8	0.45	3.4	158	1.8	33.8	-17.5
7	C1–Ti₂	BN	1.6	10	5	0.51	6.1	447	2.5	19.5	-24.0
8	C1–Ti₂	BN₂	1.6	5	5	0.44	5.3	325	2.2	27.4	-22.6
9 ^e	Ti₁	BN	1.6	10	5	0.82	9.8	738	2.5	15.9	-26.0
10 ^e	Ti₂	BN₂	1.6	5	5	0.61	7.3	245	2.3	19.6	-25.2

^a Polymerizations carried out on high vacuum line at 24 °C under 1.0 atm ethylene pressure. ^b Gram polymer/[(mol cationic metallocene)·atm·h]. ^c From GPC versus polystyrene standards. ^d Calculated from ¹³C NMR spectra.²² ^e Polymerizations carried out in chlorobenzene.

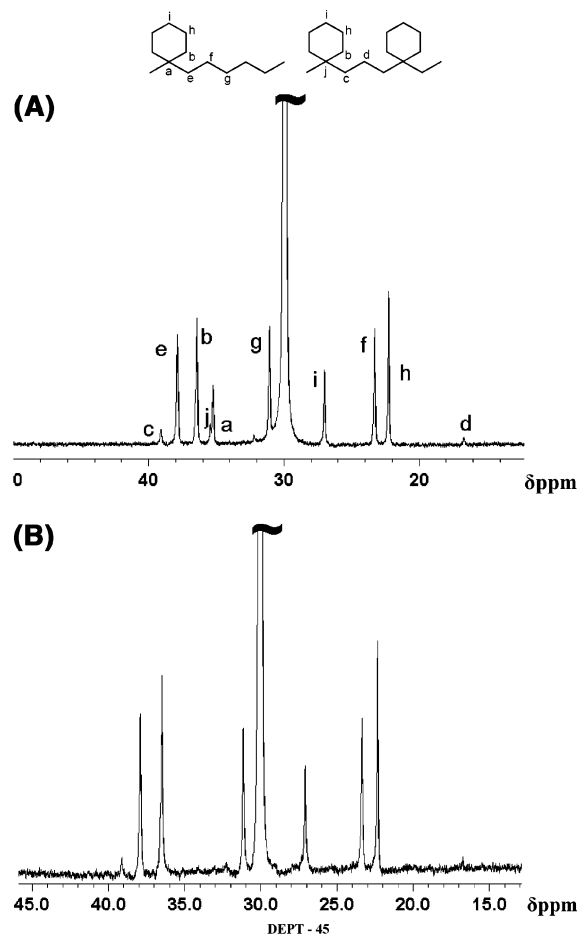


Figure 6. ¹³C NMR spectrum (100 MHz, C₂D₂Cl₄, 120 °C) of an ethylene + methylenecyclohexane copolymer showing spectral assignments: (A) sample of Table 7, entry 7; (B) sample of Table 7, entry 7, DEPT spectrum.

analog, while entry 6 versus 5 indicates that, when the incorporation level reaches ~30%, the binuclear catalyst/cocatalyst achieves only ~1.4 times greater incorporation selectivity than the mononuclear analogue. This saturation effect doubtlessly reflects the high percentage of microstructure at this point having comonomers separated by single ethylene units and the severe steric and kinetic constraints on further isoalkene enrichment. The observed absence of microstructure with adjacent incorporated comonomer units reflects the steric impediments of the bulky comonomer, and thus, in principle, the maximum readily achievable comonomer incorporation level is ~50% (the absence of C–C diads precludes accurate estimation of monomer reactivity ratios based on NMR data).

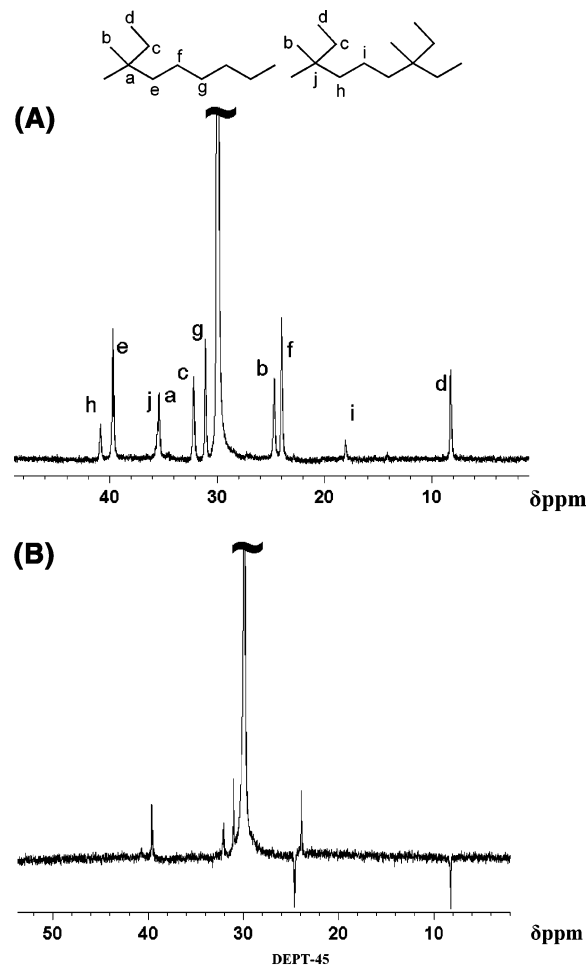


Figure 7. ¹³C NMR spectrum (100 MHz, C₂D₂Cl₄, 120 °C) of an ethylene + 2-methyl-2-butene copolymer showing spectral assignments: (A) sample of Table 7, entry 12; (B) Table 7, entry 11, DEPT spectrum.

To further explore the correlation between catalyst structure and polymerization behavior, methylene-bridged **C1–Ti₂** was also synthesized and employed in catalytic studies. It can be seen from entry 4 versus 8 in Table 8 that **C1–Ti₂** + **BN₂** incorporates ~1.4 times more methylenecyclopentane than does **Ti₂** + **BN₂**, presumably because the diminished achievable Ti–Ti distance enhances cooperative effects and increases the comonomer enchainment selectivity (see more below).²³

To investigate the role of ion pairing on the observed nuclearity effects, the more polar solvent, chlorobenzene²⁴ ($\epsilon = 5.68$), was used as the copolymerization medium (Table 8, entries 9 and 10). It can be seen that, in C₆H₅Cl, the binuclear

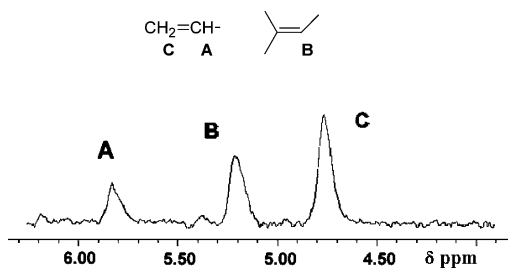
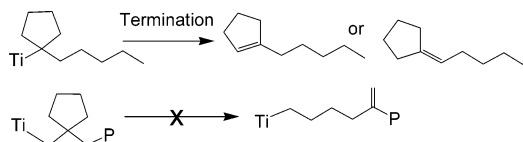


Figure 8. ^1H NMR spectrum (400 MHz, $\text{C}_2\text{D}_2\text{Cl}_4$, $120\text{ }^\circ\text{C}$) of an ethylene + methylenecyclopentane copolymer (sample of Table 7, entry 3) in the olefinic endgroup region, showing spectral assignments.

Scheme 5. Ethylene + Methylenecyclopentane (C) Copolymerization Chain Termination Pathway



$\text{Ti}_2 + \text{BN}_2$ catalyst incorporates only ~ 1.2 times more **C** than mononuclear $\text{Ti}_1 + \text{BN}$, compared with ~ 2.5 times enhancement observed in entry 1 versus 4 in Table 8. Thus, the binuclear enhancement of comonomer enchainment is significantly diminished in the more polar, ion pairing weakening solvent. The copolymerization activities in $\text{C}_6\text{H}_5\text{Cl}$ are increased moderately versus those in toluene, in sharp contrast to the significant activity enhancement in $\text{C}_6\text{H}_5\text{Cl}$ reported before for CGCZr catalysts.^{4a}

In regard to chain transfer pathways, the ^1H spectrum of the ethylene + methylenecyclopentane copolymer (Figure 8) indicates that there are two types of detectable endgroups. One set is a vinyl group (peaks A and C; because of the high M_w , the peaks are somewhat broad and peak splitting is not resolved),^{9a,25} likely derived from β -H transfer when the last inserted monomer is ethylene. The other endgroup is a trisubstituted double bond (peak B), assignable to the product of methylenecyclopentane 2,1-insertion, followed by β -H elimination, as shown in Scheme 5 (assignment based on the model compound 1-ethyl-1-cyclopentene^{22b}). When methylenecyclopentane undergoes 1,2-insertion, such chain termination processes cannot occur due to the lack of a β -H and a thermodynamically favorable β -C transfer ring-opening pathway. Thus, methylenecyclopentane 1,2-insertion can be followed by chain propagation. However, when 2,1-insertion errors occur, presum-

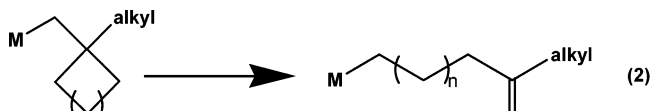
ably due to steric constraints, the next monomer (either ethylene or **C**) insertion is unfavorable, and chain termination becomes a competitive pathway, thus plausibly affording the observed trisubstituted double bond endgroup. The aforementioned observation of the absence of adjacent enchaind comonomer units (no enchaind regioerrors) also supports the above mechanism. Landis reported a similar observation in terms of the relationship between insertion regioerrors and chain termination in 1-hexene polymerization; essentially every insertion regioerror is committed to chain termination.²⁶

The ethylene + **C** copolymers are amorphous and exhibit a single glass transition temperature (T_g), as measured by DSC (Table 8). T_g values are observed between -17 and $-33\text{ }^\circ\text{C}$.

As a reference, T_g is $-73\text{ }^\circ\text{C}$ for polyisobutene and $-93\text{ }^\circ\text{C}$ for amorphous polyethylene,^{9a,27} while the T_g values of the present copolymers are higher than those of ethylene–isobutene copolymers at comparable molecular weights and comonomer incorporation levels,²⁸ reflecting the influence of the bulky enchaind rings.¹⁰ It is found that T_g increases as the comonomer incorporation level increases, reasonably because there is a greater proportion of more ordered alternating microstructures at higher comonomer incorporation levels, thus leading to higher T_g values,²⁹ in agreement with previous observations on ethylene + isobutene copolymers.²⁸

Discussion

I. Sterically Encumbered Methylenecycloalkane Copolymerization. Compared with our previously reported methylenecyclopropane (**A**) and methylenecyclobutane (**B**) ring-opening polymerization processes,^{7b} the methylenecycloalkanes investigated here, methylenecyclopentane (**C**) and methylenecyclohexane (**D**), both follow ring-unopened insertion pathways. The different polymerization pathways can be most readily ascribed to the differences in ring strain energies of the different monomers. Thus, **A** and **B** have sizable ring strain energies, which would be released in chain propagation via a ring-opening process. For those monomers with less or no strain energy, such as **C** and **D**, the ring-opening pathway is a thermodynamically unfavorable process (eq 2).



$n = 0$,	$\Delta H \sim -14\text{ kcal/mol}$
$n = 1$,	$\Delta H \sim -13\text{ kcal/mol}$
$n = 2$,	$\Delta H \sim +6.3\text{ kcal/mol}$
$n = 3$,	$\Delta H \sim +13\text{ kcal/mol}$

These reactions can be analyzed in terms of a normal β -alkyl elimination reaction, a reverse of C=C bond insertion, which is therefore estimated to be $\sim 13\text{ kcal/mol}$ endothermic,^{7c,30}

- (23) The corresponding Zr analogue C1-Zr_2 exhibits greater 1-hexene incorporation selectivity than does C2-Zr_2 , and the crystal structures of the different bridged precatalysts show the minimum possible metal–metal distance in the methylene-bridged complex is $\sim 1.3\text{ \AA}$ shorter than in the $-\text{CH}_2\text{CH}_2-$ bridged analogue, presumably facilitating the cooperative enchainment effects. Li, H.; Stern, C. T.; Marks, T. J. *Macromolecules*, in press.
- (24) Light alkenes have similar solubilities in toluene and chlorobenzene. For example, the solubility of ethylene is reported to be 0.117 mol/L in toluene^{24g} and 0.118 mol/L in chlorobenzene^{24h} under the present polymerization conditions ($25\text{ }^\circ\text{C}$, 1 atm). (a) Yang, S. H.; Huh, J. H.; Jo, W. H. *Macromolecules* **2005**, *38*, 1402–1409. (b) Chen, M.-C.; Roberts, J. A. S.; Marks, T. J. *J. Am. Chem. Soc.* **2004**, *126*, 4605–4625. (c) Forlini, F.; Tritto, I.; Locatelli, P.; Sacchi, M. C.; Piemontesi, F. *Makromol. Chem. Phys.* **2000**, *201*, 401–408. (d) Forlini, F.; Tritto, I.; Locatelli, P.; Sacchi, M. C.; Piemontesi, F. *Makromol. Chem. Phys.* **2000**, *201*, 401–408. (e) Kleinschmidt, R.; Griebenow, Y.; Fink, G. *J. Mol. Catal. A-Chem.* **2000**, *157*, 83–90. (f) Coevoet, D.; Cramail, H.; Deffieux, A. *Makromol. Chem. Phys.* **1999**, *200*, 1208–1214. (g) Atiqullah, M.; Hammawa, H.; Hamid, H. *Eur. Polym. J.* **1998**, *34*, 1511–1520. (h) Sahgal, A.; La, H. M.; Hayduk, W. *Can. J. Chem. Eng.* **1978**, *56*, 354–357.
- (25) Silverstein, R. M.; Bassler, G. C.; Morrill, T. C. *Spectrometric Identification of Organic Compounds*, 5th ed.; Wiley: New York, 1991; pp 215, 237–238.

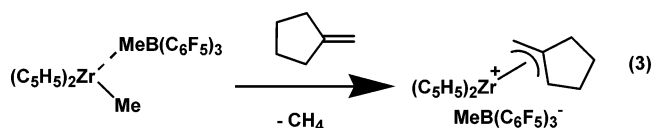
(26) Liu, Z.; Somsook, E.; White, C. B.; Rosaaen, K. A.; Landis, C. R. *J. Am. Chem. Soc.* **2001**, *123*, 11193–11207.

(27) (a) Brandrup, J.; Immergut, E. H. Eds. *Polymer Handbook*, 2nd ed.; Wiley: New York, 1975; Chapter 111, pp 143–144, and also, for PE, Chapter V, p 16. (b) Ferry, J. D. *Viscoelastic Properties of Polymers*, 2nd ed.; Wiley: New York, 1970; Tables 12–111.

(28) Shaffer, T. D.; Canich, J. M.; Squire, K. R. *Macromolecules* **1998**, *31*, 5145–5147. Here, ethylene + isobutene copolymerizations mediated by a N-modified mononuclear CGCTi catalyst result in significant isobutene enchainment in cases where the feed is very isobutene-rich (isobutene: ethylene up to 150:1).

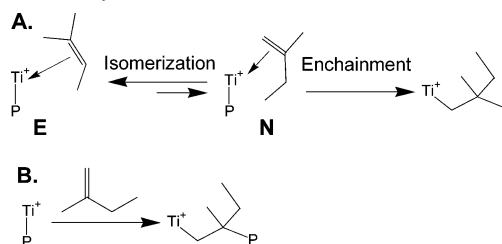
coupled with release of the cycloalkane ring strain (27, 26, 6.5, and 0 kcal/mol for cyclopropane, cyclobutane, cyclopentane, and cyclohexane, respectively).³¹ Hence, the net result is $\Delta H \sim 13 + (-27) \sim -14$; $13 + (-26) \sim -13$; $13 + (-6.5) \sim +6.5$; and $+13$ kcal/mol in these cases for $n = 0-3$, respectively (eq 2).

For monomers **C** and **D**, different catalysts lead to different catalytic products. It has been reported that $(C_5H_5)_2ZrMe^+MeB(C_6F_5)_3^-$ initially undergoes reaction with monomer **C** to form an η^3 -allyl complexes, as in eq 3,³² without insertion. We previously reported that, with $(C_5H_5)_2ZrMe^+MeB(C_6F_5)_3^-$ as the catalyst, **C** and **D** are eventually converted to the thermodynamically more stable internal olefins **I** and **J**.^{7b} When $CGCZr^+$ catalysts are employed, the same isomerization reactions occur to again yield internal olefins **I** and **J** as products. When **C** or **D** and ethylene are both present, neither $(C_5H_5)_2ZrMe^+MeB(C_6F_5)_3^-$ nor $CGCZr^+$ catalysts are capable of incorporating the comonomer into the polymer backbone, while when $CGCTi^+$ catalysts are used, ring-unopened copolymers **K** and **L** are produced. This difference in the catalytic comonomer incorporation selectivity was previously observed in our work on isobutene copolymerization: $CGCTi^+$ catalysts incorporate significant quantities of isobutene into polyethylene backbones, while $CGCZr^+$ catalysts do not. One plausible argument is that tighter ion pairing in $CGCZr$ versus $CGCTi$ structures³³ leads to lower reactivity in terms of bulky comonomer enchainment.



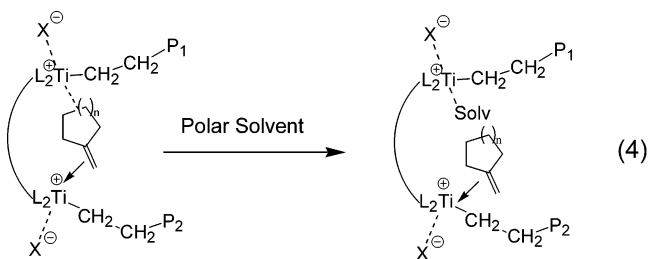
II. Sterically Encumbered 1,1,2-Trisubstituted Isoalkene Copolymerization. In the copolymerization of ethylene and 2-methyl-2-butene, only excess comonomer, 2-methyl-2-butene (**E**), is detected in the reaction mixture mother liquor after removal of the polymeric product by filtration, with no 2-methyl-1-butene (**N**) isomerization product detected. From a thermodynamic point of view, **E** is more stable than **N** by ~ 1.8 kcal/mol,³⁴ and the $E \rightleftharpoons N$ equilibrium therefore lies to the left, as in Scheme 6. Nevertheless, if there is rapid $E \rightleftharpoons N$ equilibration and **N** is much more reactive with respect to enchainment than **E**, it will be captured and inserted selectively, with all of the **E** draining away through **N**. Thus, if **E** were activated at the catalyst center and enchainment under the normal reaction conditions, the observed **N**-derived microstructure would be formed. To further confirm the above suggested pathway, **N** was examined as comonomer in ethylene copolymerization. The ¹³C NMR spectrum of the copolymer produced from ethylene + **N** is indistinguishably derived from ethylene + **E**, further supporting the proposed mechanism (Scheme 6).

Scheme 6. Ethylene + 2-Methyl-2-butene (**E**) Copolymerization Insertion Pathway



III. Binuclear Catalyst/Cocatalyst Enhancement of Comonomer Enchainment.

Among the three comonomers investigated, under identical reaction conditions, binuclear catalysts $Ti_2 + BN_2$ and $C1-Ti_2 + BN_2$ incorporate significantly greater levels of comonomer than does the mononuclear $Ti_1 + BN$ analogue, and a shorter bridge connecting the two Ti centers enhances the binuclear effects. It is plausible that the coordination of comonomer to a cationic metal center is stabilized by secondary, possibly agostic interactions,³⁵ with the proximate cationic metal center, which may facilitate/stabilize comonomer capture/binding and enhance the subsequent enchainment probability. It is likely that olefin insertion proceeds via reversible alkene association at such electrophilic catalytic centers, followed by irreversible migratory insertion, and in such a two-step process, the alkene association equilibrium constant strongly depends on cocatalyst and alkene structure as well as solvent.³⁶⁻³⁸ We suggest that the adjacent cationic metal center in the binuclear catalysts displaces the bulky comonomer coordination/dissociation equilibrium to the right, while the rate constant for coordinated comonomer migratory insertion may be comparable for mononuclear and binuclear catalysts (e.g., Scheme 7).³⁶ It has also been reported that polar solvents can compete for/coordinate to electrophilic metal centers and weaken/replace agostic interactions,³⁹ which are proposed here to be central to the observed binuclear effects. The present copolymerization results in a more polar, ion pair weakening medium²⁴ suggest the proposed agostic interactions can also be weakened by polar C_6H_5Cl (eq 4).

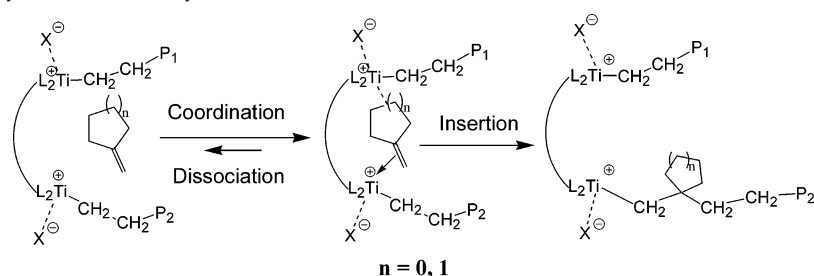


Summary

We have synthesized and characterized the binuclear organotitanium “constrained geometry catalysts” (CGCs) (μ -CH₂-

(29) Johnston, N. W. *J. Macromol. Sci., Rev. Macromol. Chem.* **1976**, *C14*, 215–250.
 (30) (a) King, W. A.; Marks, T. J. *Inorg. Chim. Acta* **1995**, *229*, 343–354. (b) Schock, L. E.; Marks, T. J. *J. Am. Chem. Soc.* **1988**, *110*, 7701–7715.
 (31) (a) Isaacs, N. S. *Physical Organic Chemistry*; Wiley: New York, 1987; pp 282–291. (b) McMillan, D. F.; Golden, D. M. *Annu. Rev. Phys. Chem.* **1982**, *33*, 493–532. (c) Benson, S. W. *Thermochemical Kinetics*, 2nd ed.; Wiley: New York, 1976; appendix.
 (32) Horton, A. D. *Organometallics* **1996**, *15*, 2675–2677.
 (33) Luo, L.; Marks, T. J. in ref 3e, pp 97–106.
 (34) Lide, D. R.; Kehiaian, H. V. *CRC Handbook of Thermophysical and Thermochemical Data*; CRC Press: Boca Raton, FL.

(35) (a) Scherer, W.; McGrady, G. S. *Angew. Chem., Int. Ed.* **2004**, *43*, 1782–1806. (b) Proscenc, M. H.; Brintzinger, H. H. *Organometallics* **1997**, *16*, 3889–3894. (c) Grubbs, R. H.; Coates, G. W. *Acc. Chem. Res.* **1996**, *29*, 85–93. (d) Proscenc, M. H.; Janiak, C.; Brintzinger, H. H. *Organometallics* **1992**, *11*, 4036–4041. (e) Cotter, W. D.; Bercaw, J. E. *J. Organomet. Chem.* **1991**, *417*, C1–C6. (f) Krauledat, H.; Brintzinger, H. H. *Angew. Chem., Int. Ed. Engl.* **1990**, *29*, 1412–1413. (g) Piers, W. E.; Bercaw, J. E. *J. Am. Chem. Soc.* **1990**, *112*, 9406–9407. (h) Brookhart, M.; Green, M. L. H.; Wong, L. L. *Prog. Inorg. Chem.* **1988**, *36*, 1–124. (i) Clawson, L.; Soto, J.; Buchwald, S. L.; Steigerwald, M. L.; Grubbs, R. H. *J. Am. Chem. Soc.* **1985**, *107*, 3377–3378.

Scheme 7. Binuclear Catalysts Facilitate Bulky Comonomer Enchainment

CH₂-3,3'){(η⁵-indenyl)[1-Me₂Si('BuN)](TiMe₂)₂} [EBICGC-(TiMe₂)₂; **Ti**₂] and (μ-CH₂-3,3'){(η⁵-indenyl)[1-Me₂Si('BuN)](TiMe₂)₂} [EBICGC(TiMe₂)₂; **C1-Ti**₂] together with the bifunctional bisborane activator 1,4-(C₆F₅)₂BC₆F₄B(C₆F₅)₂ (**BN**) for ethylene + hindered isoalkene copolymerization processes. Specifically examined are the poorly responsive comonomers

1,1-disubstituted isobutene, methylenecyclopentane, methylenecyclohexane, and 1,1,2-trisubstituted 2-methyl-2-butene. For the latter three comonomers, we report for the first time that these can be incorporated in large percentages into polyethylene backbones via coordination polymerization processes. Large increases in comonomer enchainment efficiency into the polyethylene microstructure are observed versus the corresponding mononuclear catalyst [1-Me₂Si(3-ethylindenyl)('BuN)]TiMe₂ (**Ti**₁) + B(C₆F₅)₃ (**BN**) under identical polymerization conditions. Solvent polarity also plays significant role in binuclear ion pairing and in comonomer enchainment selectivity.

- (36) (a) Casey, C. P.; Tunge, J. A.; Lee, T.-Y.; Fagan, M. A. *J. Am. Chem. Soc.* **2003**, *125*, 2641–2651. (b) Landis, C. R.; Rosaaen, K. A.; Uddin, J. *J. Am. Chem. Soc.* **2002**, *124*, 12062–12063. (c) Casey, C. P.; Lee, T.-Y.; Tunge, J. A.; Carpenetti, D. W., II. *J. Am. Chem. Soc.* **2001**, *123*, 10762–10763. (d) Grubbs, R. H.; Coates, G. W. *Acc. Chem. Res.* **1996**, *29*, 85–93.
- (37) (a) Stoebenau, E. J., III; Jordan, R. F. *J. Am. Chem. Soc.* **2004**, *126*, 11170–11171. (b) Stoebenau, E. J., III; Jordan, R. F. *J. Am. Chem. Soc.* **2003**, *125*, 3222–3223. (c) Carpentier, J.-F.; Maryin, V. P.; Luci, J.; Jordan, R. F. *J. Am. Chem. Soc.* **2001**, *123*, 898–909.
- (38) Brandow, C. G.; Mendiratta, A.; Bercaw, J. E. *Organometallics* **2001**, *20*, 4253–4261.
- (39) (a) Bouwkamp, M. W.; de Wolf, J.; del Hierro Morales, I.; Gercama, J.; Meetsma, A.; Troyanov, S. I.; Hessen, B.; Teuben, J. H. *J. Am. Chem. Soc.* **2002**, *124*, 12956–12957. (b) Kawabe, M.; Murata, M. *Macromol. Chem. Phys.* **2001**, *202*, 2440–2446. (c) Rybtchinski, B.; Konstantinovskiy, L.; Shimon, L. J. W.; Vigalok, A.; Milstein, D. *Chem.-Eur. J.* **2000**, *6*, 3287–3292. (d) Carr, N.; Mole, L.; Orpen, A. G.; Spencer, G. L. *J. Chem. Soc., Dalton Trans.* **1992**, *18*, 2653–2662. (e) Peng, T. S.; Gladysz, J. A. *J. Am. Chem. Soc.* **1992**, *114*, 4174–4181. (f) Agbossou, S. K.; Bodner, G. S.; Patton, A. T.; Gladysz, J. A. *Organometallics* **1990**, *9*, 1184–1191. (g) Schmidt, G. F.; Brookhart, M. *J. Am. Chem. Soc.* **1985**, *107*, 1443–1444.

Acknowledgment. This research was supported by grants from NSF (CHE-0415407) and DOE (86ER13511). L.L. thanks Dow Chemical Company for a postdoctoral fellowship. We thank Dr. J. Wang for helpful discussions.

Supporting Information Available: Details of catalyst, co-catalyst syntheses, polymerization experiments, and crystal structures. This material is available free of charge via the Internet at <http://pubs.acs.org>.

JA052995X